学位論文

Studies on the role of a mitochondrial protein GC1 in the regulation of Ras-PI3K signaling-mediated endocytosis

(Ras-PI3K シグナルを介したエンドサイトーシス制御機構におけるミトコンドリアタンパク質 GC1 の役割に関する研究)

2019 年 9 月

北海道大学

ネパル プラバ

Nepal Prabha

学位論文

Studies on the role of a mitochondrial protein GC1 in the regulation of Ras-PI3K signaling-mediated endocytosis

(Ras-PI3K シグナルを介したエンドサイトーシス制御機構におけるミトコンドリアタンパク質 GC1 の役割に関する研究)

2019 年 9 月

北海道大学

ネパル プラバ

Nepal Prabha

TABLE OF CONTENTS

LIST OF PUBLICATIONS AND PRESENTATIONS

List of publications

Prabha Nepal, Yoichiro Fujioka, Aiko Yoshida, Aya O. Satoh, Paudel Sarad, Hitoshi Sasajima, and Yusuke Ohba. The mitochondria glutamate carrier protein 1 negatively regulates clathrin-independent endocytosis and endosome maturation. Molecular Cell, in submission.

List of presentations

Prabha Nepal, Yoichiro Fujioka, Aya O. Satoh, Kosui Horiuchi, Sarad Paudel, Sayaka Kashiwagi, Aiko Yoshida, Mari Fujioka, Asuka Nanbo and Yusuke Ohba. Role of inner mitochondrial membrane proteins in the regulation of endocytosis mediated by Ras-PI3K signaling. Joint Annual Meeting of Japanese Society of Developmental Biology (51^{st}) and Japanese Society of Cell Biology (70^{th}), June 5-8, 2018, Tokyo, Japan.

SUMMARY

[Background and Objectives]

The small GTPase Ras plays a key role in the variety of cellular functions through a spatiotemporal control of effector activation. The GTP-bound, active form of Ras interacts with the Ras-binding domain (RBD) of the effector molecules, which include phosphoinositide 3-kinase (PI3K), c-Raf serine threonine kinase, and Ral guanine nucleotide dissociation stimulator (RalGDS). Using the bimolecular fluorescence complementation (BiFC) technique, our laboratory has previously reported that different from the complexes of Ras-Raf and Ras-RalGDS, the Ras-PI3Kp110γ (Class IB PI3K catalytic subunit gamma isoform) complex specifically translocates from the plasma membrane to endosomes upon epidermal growth factor (EGF) stimulation, and resulted in the activation of Ras-PI3K complex on the endosome. In addition, colleagues in our laboratory have revealed that Ras-PI3K signaling from the endosomes promotes clathrin-independent endocytosis and endosomal maturation. The question to be addressed is what gives rise to the localization of the Ras-PI3K complexes in the endosome. Our laboratory has identified a 28-amino-acid-long sequence that is specifically found in RBD of PI3K, but not in those of Raf and RalGDS, and revealed that this peptide is involved in the translocation of the Ras-PI3K complex to the endosome. The peptide was named RAPEL after Ras-PI3K endosomal localization. Through the screening of RAPEL-binding factors with the use of yeast two-hybrid system and immunoprecipitation followed by mass spectrometry, 48 potential binding proteins to RAPEL have been isolated. To my surprise, among these factors, several mitochondrial proteins have been identified. In this study, I focused on one of these mitochondrial membrane proteins, glutamate carrier 1 (GC1), a glutamate-proton symporter, and aimed to evaluate its role in endocytosis.

[Materials and Methods]

The interaction of GC1 with RAPEL was evaluated by immunoprecipitation and immunoblotting. The coding sequence of GC1 was obtained from a cDNA library of 293T cells and those of truncation mutants were prepared by PCR with the use of primer sets for respective fragments. These coding sequences were subcloned into the restriction enzyme recognition sites of expression vectors for the proteins tagged with epitopes, including fluorescent proteins. Such expression vectors or others that had been developed in our laboratory were transfected into cells according to the manufactures' recommendations.

Immunofluorescence analysis was performed by a common procedure. The cells either expressing fluorescent-tagged proteins or being subjected to immunofluorescence were observed under wide-field epi-fluorescence microscopy or confocal microscopy. The localization of GC1 in the inner and outer mitochondrial membranes was evaluated by mega-mitochondria method using valinomycin, a reagent that triggers mitochondrial swelling and makes it possible to distinguish the inner and outer membranes of mitochondria by confocal microscopy. Knockdown experiments were carried out by introducing small interfering RNA (siRNA) against the GC1 into cells. The knockdown efficacy was determined at a mRNA level and a protein level by quantitative PCR (48 hours after transfection) and immunoblotting (after 72 hours), respectively. Endocytic activities of cells were evaluated by quantifying the uptake of fluorescently labeled dextran and transferrin, which are incorporated into the cells through clathrin-independent and clathrin-dependent endocytosis, respectively. Endosomal acidification was examined by labeling and tracking acidic vesicles using fluorescent probe, LysoTracker® Red DND-99. The acquired images were quantified and analyzed by using MetaMorph software. Other biochemical analyses, including immunoprecipitation, were performed as described elsewhere.

[Results]

I revealed that GC1 interacted with RAPEL by an immunoprecipitation method and its localization in the mitochondria was confirmed by an immunofluorescence analysis as well as live-cell imaging for cells expressing fluorescent protein-tagged GC1. GC1-positive mitochondria are localized in close proximity with Ras-PI3K complex-positive endosomes. These results strengthened a hypothesis that endosomes may interact with mitochondria through the binding between GC1 and Ras-PI3K complex. However, to interact with the cytosolic or endosomal PI3K, GC1 needs to be localized at the mitochondrial outer membrane. As far as I am aware, there are no reports about its localization in the outer mitochondrial membrane. Therefore, I evaluated submitochondrial localization of GC1 with mega-mitochondria method and demonstrated that GC1 was localized not only in the inner membrane as reported previously, but also in the outer membrane of mitochondria, further suggesting the direct interaction of GC1 with RAPEL. Assay with truncated mutants of GC1 revealed that its N-terminal half was responsible for RAPEL binding whereas the C-terminal half was for mitochondrial localization. Live-cell imaging demonstrated that GC1 negatively regulates the translocation of the Ras-PI3K complex to the endosome. Transferrin and dextran uptake assays demonstrated that GC1 positively and negatively regulates clathrin-dependent

and -independent endocytosis, respectively. Given that GC1 functions as a symporter of glutamate and proton and Ras-PI3K signaling is reported to be involved in endosomal maturation, I hypothesized that GC1 might play a role in endosomal maturation. In fact, assay with the fluorescent probe for acidic organelles in living cells revealed that GC1 negatively regulates endosome acidification and delayed endosome maturation. These results together demonstrated that GC1 plays two-sided roles in the regulation of endocytosis.

[Discussion]

In this study, I revealed that the mitochondrial protein GC1 interacts with RAPEL and negatively regulates endosomal translocation of the Ras-PI3K complex from the plasma membrane, clathrin-independent endocytosis, and endosomal maturation. Another important finding is that GC1 positively regulates clathrin-dependent endocytosis. The negative role of GC1 in the regulation of endosomal maturation might be accounted for by the function of GC1 as a proton transporter; i.e., possibly from cytosol to mitochondria; a local decrease in cytosolic proton due to pumping proton into the mitochondria by activated GC1 to a decrease in proton transport into the endosome, which results in the delay in endosome maturation. However, many questions remain to be addressed. For example, it is unknown whether the interaction of GC1 with RAPEL is direct or indirect. In addition, the direction of proton/glutamate flux at the endosome-mitochondria contact sites are yet to be investigated. Since clathrin-dependent pathway is reported to be independent of Ras-PI3K signaling, it is possible that GC1 plays a role in the “pathway switching” between clathrin-dependent and clathrin-independent endocytosis.

GC1 has been reported to be associated with neurological disorder like epilepsy, some types of which are related with the dysfunction of endocytosis: namely, mutation in dynamin, a key regulator of clathrin-dependent endocytosis. Therefore, it might be possible that GC1 might participate in the pathogenesis of epilepsy not only through glutamate transport, but also through the regulation of clathrin-dependent endocytosis, albeit in part, although the detailed molecular mechanism has yet to be determined. In addition, GC1 is revealed to upregulate proliferation and migration of colorectal cancer cells with K-Ras mutation by promoting glutamine synthesis. It has been reported that endocytosis suppress cancer cell proliferation and invasion so it might be possible for GC1 to promote cancer cell malignancy thorough the regulation of membrane trafficking. Thus, it might be worth exploring the involvement of GC1 in pathophysiological conditions, including endocytosis-related diseases in the future.

[Conclusion]

In this study, I have demonstrated that:

- GC1, a mitochondrial membrane protein, interacts with RAPEL of PI3K
- GC1 negatively regulates translocation of Ras-PI3K complex from the plasma membrane to the endosome
- GC1 negatively regulates clathrin-independent endocytosis and endosomal acidification
- GC1 positively regulates clathrin-dependent endocytosis but the mechanism is still unknown

To the best of my knowledge, there are no reports so far on the role of GC1 in the endocytic process; therefore, this is the first study carried out to demonstrate its role in endocytosis. I hereby provide a novel function of GC1 as a regulator of clathrin-independent endocytosis through regulating the Ras-PI3K signaling.

LIST OF ABBREVIATIONS

ANOVA: one-way analysis of variance

ANT: adenine nucleotide translocator

ATP: adenosine triphosphate

BiFC: bimolecular fluorescence complementation

BSA: bovine serum albumin

CFP: cyan fluorescent protein

DMEM: Dulbecco's modified Eagle's medium

EDTA: ethylenediaminetetraacetic acid

EEA-1: early endosome antigen-1

EGF: epidermal growth factor

ER: endoplasmic reticulum

ERK1/2: extracellular signal-regulated kinase 1/2

FBS: fetal bovine serum

FRET: Förster resonance energy transfer

GAP: GTPase-activating protein

GAPDH: glyceraldehyde 3-phosphate dehydrogenase

GC1: glutamate carrier 1

GEF: guanine nucleotide exchange factors

GFP: green fluorescent protein

GST: glutathione S-transferase

HA: hemagglutinin

HRP: horseradish peroxidase

LB: lysogeny broth

MAM: mitochondria-associated membrane

MANOVA: multivariate analysis of variance

MAPK: mitogen-activated protein kinase

MCS: membrane contact sites

NCBI: National Center for Biotechnology Information

PBS: phosphate-buffered saline

PCR: polymerase chain reaction

PEI: polyethylenimine

PI3K: phospoinositide 3-kinase

PVDF: polyvinylidene difluoride

qPCR: quantitative PCR

RalGDS: Ral guanine nucleotide dissociation stimulator

RAPEL: Ras-PI3K endosomal localization

RBD: Ras-binding domain

RFP: red fluorescent protein

SDS-PAGE: sodium dodecyl sulfate polyacrylamide gel electrophoresis

SECFP: super enhanced CFP

s.e.m.: standard error mean

siRNA: small interfering RNA

SLC: mitochondria solute carrier

TBS: Tris-buffered saline

TBS-T: TBS containing polyethylene glycol (20) sorbitan monolaurate (TWEEN®20)

TCL: total cell lysate

TMRM: tetramethylrhodamine methyl ester

TrkA: tropomyosin receptor kinase A

V-ATPase: vacuolar H^+-ATPase

VDAC2: voltage-dependent anion channel 2

INTRODUCTION

Endocytosis, a fundamental cellular process, is utilized by all the living cells to internalize different molecules into the cells (Mayor and Pagano, 2007). There are two categories of endocytosis: phagocytosis (cell eating) and pinocytosis (cell drinking), depending upon the types of substances internalized into the cells and their mechanisms. Phagocytosis occurs only in specific mammalian cells such as monocytes, neutrophils, and macrophages. Phagocytosis is a highly active and greatly regulated endocytosis that comprises cell-surface specific receptors and signaling cascades regulated by Rho-family GTPases (Hall and Nobes, 2000). In contrast, pinocytosis is basically observed in all the cell contexts, and categorized into four basic types: macropinocytosis, clathrin-dependent endocytosis, caveolae-dependent endocytosis, and clathrin-and caveolae-independent endocytosis (Conner and Schmid, 2003). In general, all pathways proceed with the following steps: First, to uptake substances, the plasma membrane forms invaginations or protrusions leading to the appearance of newly formed vesicles into the cytoplasm. The internalized vesicles gradually mature into early endosomes, late endosomes, and lysosomes. During the maturation process, uptake of proton (H^+) into the vesicles is increased by vacuolar H^+-ATPase (V-ATPase), which is an endosomal membrane protein. Finally, the substances inside the lysosomes are degraded by the lysosomal enzymes, which are activated in acidic environment. A part of internalized substances such as receptors are recycled back to the plasma membrane by passing through early endosomes and finally through recycling endosomes.

Membrane trafficking of the internalized vesicles within the cells is regulated by various proteins such as Rab GTPases, tethering molecules, and SNARE proteins, which promote membrane fusion (Huotari and Helenius, 2011). Rab5 is a major membrane component of early endosomes (Huotari and Helenius, 2011), and recruits a range of effector molecules to the endosomal membrane. Among them, the tethering protein early endosome antigen-1 (EEA-1) helps endocytic vesicles to fuse with early endosomes (Christoforidis et al., 1999). During the maturation of early endosomes, Rab7 is recruited to their membranes by Rab5, which leads to the temporary formation of Rab5/Rab7 double-positive endosomes. The removal of Rab5 and its substitution with Rab7 is a crucial step in the formation of late endosomes and in the transport of the cargo into the lysosomes (Huotari and Helenius, 2011).

Endosome has been traditionally considered as an organelle that is in charge of intracellular trafficking of endocytosed cargos; however, growing evidence supports that the endosome functions not only as a cargo container but also as a signaling platform (Murphy et al., 2009).

Furthermore, depending on where the signaling molecules localize, they induce different cellular functions. For example, in neuronal cells, a transient signal from the nerve growth factor-bound tropomyosin receptor kinase A (TrkA) receptor at the plasma membrane promotes proliferation, whereas lasting signal from the TrkA receptor in endosomes induces differentiation (Ascano et al., 2012). Thus, the same signaling molecules can spatiotemporally regulate different cellular phenomena by controlling "when" and "where" they emit the signal.

Ras proteins are small GTPases that regulate a variety of signal transduction processes through the activation of different effector molecules. The Ras subfamily consists of three members: homolog of Harvey rat sarcoma virus (H-Ras), homolog of Kristen rat sarcoma virus (K-Ras), and Ras derived from neuroblastoma (N-Ras). These three classes of Ras share 80% identity in their amino acid sequences (Boguski and McCormick, 1993; Castellano and Santos, 2011). Ras proteins cycle between two states, a GTP-bound active form and a GDP-bound inactive form (Bos, 1997; Downward, 1992). The inactive form of Ras is transformed into the active form by guanine nucleotide exchange factors (GEFs). Only the active form of Ras can bind to effector molecules and transmit signals. The active form gets back to the inactive form by hydrolysis of bound GTP, which is mediated by GTPase-activating proteins (GAPs). Mutations in Ras are frequently found in various human malignant tumors, including bladder cancers and adrenal cancers for H-Ras, pancreatic cancers and colorectal cancers for K-Ras, and lymphomas and melanomas for N-Ras (Prior et al., 2012). Ras with such mutations becomes unable to be inactivated by GAPs and results in constitutive activation, which leads to aberrant activation of downstream signaling and subsequent abnormal cell proliferation. A series of post-translational modifications of CAAX motif at the very C-terminus of Ras targets this protein to membrane compartments. The AAX residue of CAAX motif is cleaved by Ras-converting CAAX endopeptidase 1, which localizes in the endoplasmic reticulum (ER), followed by conversion of the cysteine residue in CAAX into farnecylcysteine processed by farnecyltransferase (Boyartchuk et al., 1997; Hancock et al., 1989). Subsequently, the cysteine residue(s) in the C-terminal hyper variable regions, which lie at the just N-terminal side of the CAAX motif, of H-Ras and N-Ras are palmitoylated by the Ras protein acyltransferase in the Golgi apparatus, resulting in localization of Ras to the plasma membrane and other membrane compartments, including the ER and the Golgi (Prior et al., 2001; Chiu et al., 2002). K-Ras, on the other hand, is not palmitoylated but

preferentially localizes at the plasma membrane due to the basicity of its hypervariable region that is comprised of multiple lysine residues (Hancock et al., 1991).

Although Ras protein itself does not have enzymatic activity (except for the weak GTPase activity), it mediates various cellular processes, including cell differentiation, growth, survival, and motility. Such a variety of functions of Ras might be accounted for by the presence of more than ten different effector molecules, which bind to Ras through their Ras-binding domain (RBD) (Campbell et al., 1998; Lowy and Willumsen, 1993; Vojtek and Der, 1998). For example, the serine/threonine kinase Raf activates the mitogen-activated protein kinase (MAPK) pathway, which eventually leads to the enhancement of transcription, following the translocation of phosphorylated extracellular signal-regulated kinase 1/2 (ERK1/2) from the cytoplasm to the nucleus (Robbins et al., 1992; Vojtek et al., 1993). The Ral guanine nucleotide dissociation stimulator (RalGDS) activates Ral, which regulates endocytosis and transcription by interacting with downstream effectors such as RalA-binding protein 1 and ZO-1-associated nucleic acid-binding protein (Frankel et al., 2005; Nakashima et al., 1999).

Phosphoinositide 3-kinase (PI3K) is a lipid kinase that phosphorylates the 3-OH group of inositol membrane lipids and plays a vital role in various cellular processes, including cell division, growth, differentiation, and other cellular functions (Vanhaesebroeck et al., 2012). Based on the structural domains of PI3K and its substrate specificity, PI3K is divided into three different classes (I, II, and III), each class of which has different isoforms (Jean and Kiger, 2014). Our laboratory has previously reported that a complex formed between H-Ras and p110γ (Class IB PI3K catalytic subunit gamma isoform), when visualized by the bimolecular fluorescence complementation (BiFC) assay, is specifically localized in early endosomes upon epidermal growth factor (EGF) stimulation (Tsutsumi et al., 2009). In addition, this translocation of the Ras-PI3K complex from the plasma membrane to the endosome eventually promotes endocytosis, namely clathrin-independent endocytosis (Fujioka et al., 2011). Moreover, our laboratory has recently identified the amino acid sequence in PI3K that is responsible to the above-mentioned endosomal translocation of Ras-PI3K complex (Fujioka et al., 2019). This sequence has been named RAPEL after Ras-PI3K endosomal localization. Screening of RAPEL-binding factors with the yeast two-hybrid method and mass spectrometry of immunoprecipitates has identified 48 candidates, in which four mitochondrial proteins are interestingly included. These results suggest the possibility that mitochondrial proteins can interact with RAPEL and participate in the spatiotemporal regulation of Ras-PI3K complex, either directly or indirectly.

Mitochondria are the dynamic organelles with constitutive fission and fusion. Mitochondria are the major metabolic sites in cells and produce ATP. In addition to metabolism, they play an important role in Ca^{2+} signaling, lipid synthesis and transfer, and apoptosis (Mesmin, 2016; Rizzuto et al., 2012; Wang and Youle, 2009). Until recently, it has been assumed that mitochondria function alone; however, growing evidence has indicated that the interaction between mitochondria and other organelles contributes a variety of cellular functions. For example, the membrane contact site (MCS) between the mitochondria and ER, which is called a mitochondria-associated ER membrane (MAM) (Vance, 1990), is reported to play important roles in various cellular phenomena, including lipid transport from ER to mitochondria (Vance, 2014), mitochondrial fission (Friedman et al., 2013), and the formation of autophagosomal membrane (Hamasaki et al., 2013).

Several reports have demonstrated the MCS between the endosome and other organelles. For instance, division of endosome cleaved by tubular ER occurs at the MCS between the endosome and ER (Rowland et al., 2014). It is also reported that once the endosome, which contains ion-bound transferrin, interacts with mitochondria, iron ion in the endosome is transferred to the mitochondria (Das et al., 2016; Sheftel et al., 2007). As far as I am aware, these are only reports that describe the mitochondria-endosome interaction.

Recently, colleagues in our laboratory have revealed that VDAC2, one of the outer mitochondrial membrane proteins, is a RAPEL-binding protein. It positively regulates Ras-PI3K-mediated endocytosis at the mitochondria-endosome contact sites (unpublished data). Therefore, in this study, I focused on another mitochondrial protein glutamate carrier proteins 1 (GC1) and analyzed its function in the regulation of Ras-PI3K signaling-mediated endocytosis.

GC1 is a mitochondrial membrane protein that belongs to mitochondria solute carrier (SLC) family 25 which consists of more than 50 different proteins (Palmieri and Monné, 2016). All members of SLC25 have a tripartite structure consisting of 3 tandemly repeated homologous domains, each of which is composed of approximately 100 amino acid residues (Palmieri et al., 2014). Each repeat harbors the conserved characteristic motif and two hydrophobic transmembrane portions connected by a hydrophilic matrix loop (Kunji and Harding, 2003; Pebay-Peyroula et al., 2003). SLC25 proteins are folded and thereby embedded in the mitochondrial membrane as 6 transmembrane proteins (Kunji and Harding, 2003; Pebay-Peyroula et al., 2003). Even with similar structures shared among SLC25 family proteins,

they transport different substrates across the inner mitochondrial membrane (Palmieri, 2004; 2014). Such substrates include metabolites, nucleotides, and cofactors.

GCs are initially identified as members of the SLC25 family in 2002 (Fiermonte et al., 2002). There are two distinct isoforms of GCs, viz., GC1 and GC2, which are encoded by *SLC25A22* and *SLC25A18* genes, respectively, with 63% identity to each other at the amino acid level (Fiermonte et al., 2002). *In vitro* reconstitution assay using purified GCs and liposomes showed that both isoforms catalyze transport of L-glutamate, but not D-glutamate, aspartate, glutamine, and asparagine, along with H^+ or in exchange for hydroxide ion (OH^-) (Fiermonte et al., 2002). Because the mRNA level of GC1 is more abundant in almost all human tissues than that of GC2, GC1 is considered to potently play a role in glutamate transport therein (Fiermonte et al., 2002). So far, GC1 is implicated in pathogenesis of epilepsy and cancer. Loss-of-function mutations in GC1 are identified in patients with early epileptic encephalopathy or migrating partial seizures in infancy (Molinari et al., 2009; 2005; Poduri et al., 2013). Increased expression levels of GC1 are found in colorectal cancers with K-Ras mutation and osteosarcoma (Wong et al., 2016; Chen and Wu, 2018), which is implicated in the promotion of proliferation, migration/invasion, and metastasis (Wong et al., 2016). GC1 might also function under physiological conditions. For example, GC1 is involved in production in the islets; knockdown of GC1 in insulinoma INS-1E cells resulted in reduction of glucose-stimulated insulin secretion (Casimir et al., 2009). In astrocyte, GC1 is crucial for maintaining glutamate homeostasis (Goubert et al., 2017).

In this study, I examined the role of GC1 in the regulation of Ras-PI3K signaling-mediated endocytosis. GC1 was indeed found to interact with RAPEL and negatively regulates endosomal translocation of Ras-PI3K complex from plasma membrane and clathrin-independent endocytosis.

MATERIALS AND METHODS

Reagent and Antibody

Human EGF recombinant protein was purchased from PeproTech (Rocky Hill, NJ, USA). Alexa Fluor 546 or Alexa Fluor 488-labeled dextran (10 kDa), Alexa Fluor 546-labeled transferrin, Alexa Fluor 594 or Alexa Fluor 647-conjugated immunoglobulin G (IgG) secondary antibodies to mouse, rabbit, or rat, tetramethyl rhodamine methyl ester perchlorate (TMRM), and MitoTracker™ Red CMXRos were purchased from Thermo Fisher Scientific (Carlsbad, CA, USA). LysoTracker® Red DND-99 was purchased from Invitrogen Molecular Probes (Eugene, OR, USA). AcidiFluor™ ORANGE-labeled dextran was purchased from Goryo Chemical (Sapporo, Japan). Horseradish peroxidase (HRP)-labeled anti-mouse and anti-rabbit IgG secondary antibodies were obtained from GE Healthcare (Little Chalfont, UK), an HRP-labeled anti-goat IgG secondary antibody was from Promega (Madison, Wis., USA), and an anti-glutathione S-transferase (GST) antibody was from Wako Pure Chemical Industries, Ltd. (Osaka, Japan). Antibodies for green fluorescent protein (GFP), red fluorescent protein (RFP), hemagglutinin (HA) (3F10), β-actin (sc-1616), Myc-tag, and GC1 were purchased from Medical & Biological Laboratories (MBL, Nagoya, Japan), Roche (Indianapolis, IN, USA), Santa Cruz Biotechnology (Santa Cruz, CA, USA), and Abcam (Cambridge, UK), respectively. Anti-FLAG M2 antibodies were obtained from Stratagene (La Jolla, CA, USA) and Sigma-Aldrich (St Louis, MO, USA).

Cell culture

The human embryonic kidney epithelial cell line HEK293T (CRL-11268), the human cervical cancer-derived cell line HeLa (CCL-2), and the human epidermoid cancer-derived cell line A-431 (CRL-1555) were obtained from American Type Culture Collection (Manassas, VA, USA). The African green monkey-derived kidney epithelial cell line Cos-1 (JCRB9082) was purchased from Japanese Collection of Research Bioresources Cell Bank at the National Institutes of Biomedical Innovation, Health and Nutrition (Ibaraki, Osaka, Japan). These cells were cultured in Dulbecco's modified Eagle medium (high glucose) containing 10% fetal bovine serum (FBS; Life Technologies, Carlsbad, CA, USA) and 1% penicillin-streptomycin (Sigma-Aldrich) at 37°C and 5% CO_2 in a humidified atmosphere.

Transfection

Expression plasmids were transfected into the cells with Polyethylenimine (PEI) MAX 40K (Polysciences, Warrington, PA, USA) according to the manufacturer's protocol. Briefly, up to 3 μg in total of purified plasmids and 2 μl of polyethylenimine were added to 250 μl of OPTI-MEM (Life Technologies) and vortexed briefly. After incubation at room temperature for 5 minutes, the mixture was transferred to cell culture medium. After incubation for 6 hours in a CO_2 incubator, the culture medium was changed to fresh medium.

For dextran uptake assay, FuGene® HD Transfection Reagent (Roche) was used. Briefly, 1 μg purified plasmids and 3 μl of FuGene HD were added to 100 μl of OPTI-MEM, vortexed, and incubated at room temperature for 10 minutes. The mixture was then added to cell culture medium. The cells were incubated at 37°C for 6 hours and the medium was then changed to fresh medium.

Immunoblotting

Cells were lysed in an NP40 lysis buffer (10 mM Tris-HCl pH 7.4, 150 mM NaCl, 0.5% Nonidet P-40, 5 mM ethylenediaminetetraacetic acid (EDTA), 10% (v/v) glycerol, 1 mM Na_3VO_4, 1 mM phenylmethylsulfonyl fluoride, 100 mM NaF, 10 μg/ml leupeptin, 10 μg/ml aprotinin) for 30 minutes on ice. The lysates were clarified by centrifugation at 20,000 × *g* for 10 minutes at 4°C and subjected to SDS-polyacrylamide gel electrophoresis (SDS-PAGE). The separated proteins were transferred to a polyvinylidene difluoride (PVDF) membrane (Millipore, Darmstadt, Germany). The PVDF membrane was incubated with 5% skim milk in Tris-buffered saline (TBS) containing 1% polysorbate 20 [(TWEEN®) 20 (TBS-T)] for 1 hour at room temperature to block nonspecific binding of antibodies. The membrane was further incubated with primary antibodies (GST, 1:1,000; RFP, 1:1,000; HA, 1:1,000; GFP, 1:1,000; β-actin, 1:2,000; FLAG, 1:1,000; Myc-tag, 1:1,000; GC1, 1:1,000) overnight at 4°C. The PVDF membrane was washed three times with TBS-T and incubated with HRP-labeled secondary antibodies (1: 5,000) at room temperature for 1 hour with gentle shaking. After washing three times with TBS-T, the immune complexes were detected by ECL Western Blotting Detection Reagent (GE Healthcare) and analyzed with an LAS-1000 UV mini image analyzer (FUJIFILM, Tokyo, Japan).

Pull down assay

After washing cells twice with phosphate-buffered saline (PBS), the cells were solubilized in the NP40 lysis buffer and clarified by centrifugation at 20,000 × *g* for 10 minutes at 4°C. The total cell lysate (TCL) was incubated with glutathione Sepharose beads (GE Healthcare) for 1 hour at 4°C with gentle rotation. After washing three times with the NP40 lysis buffer, the proteins bound to beads were eluted in 1 × SDS sample buffer by boiling at 95°C for 5 minutes and subjected to immunoblotting. Aliquots of TCL were also analyzed by immunoblotting as a loading control.

Immunoprecipitation

TCLs prepared with the NP40 lysis buffer were incubated with an anti-HA antibody or an anti-GFP antibody for 1 hour at 4°C with gentle rotation. After addition of protein G-Sepharose beads (GE Healthcare), they were further incubated for 1 hour at 4°C. After washing with the NP40 lysis buffer, the immune complexes were recovered in 1 × SDS sample buffer by boiling for 5 minutes at 95°C. The proteins bound to beads and aliquots of TCL were subjected to immunoblotting.

RNA extraction and quantitative PCR

Total RNA was extracted using RNeasy Mini Kit (QIAGEN, Valencia, CA, USA) and cDNA was obtained by reverse transcription from 2.5 μg of the total RNA using SuperScript® VILO™ cDNA Synthesis Kit (Life Technologies). mRNA levels of each molecule were quantified with the StepOne real-time PCR system (Applied Biosystems, Foster City, CA, USA), the primer sets given in Table 1, and Power SYBR® Green PCR Master Mix (Life Technologies). The mRNA level of glyceraldehyde 3-phosphate dehydrogenase (GAPDH) was used for the internal control and the expression level of GC1 in each sample was expressed as a relative value to those in control samples.

RNA interference

Small interfering RNAs (siRNAs) (siGC1 #1 s533951, siGC1 #5 s36255, siGC1 #7 s36257) were purchased from Ambion (Austin, TX, USA). AllStars Negative Control siRNA (QIAGEN) was used for control siRNA. A431 cells were cultured in a 6-well plate (Corning, CITY, STATE, COUNTRY) at a density of 2×10^5 cells/well for 24 hours, and transfected with 25 pmol siRNA with the use of Lipofectamine

RNAiMAX (Life Technologies). The knockdown efficacy at mRNA levels was evaluated by qPCR at 48 hours after transfection and that at the protein levels was done by immunoblotting at 72 hours after transfection, respectively.

In rescue experiments, expression plasmids for the proteins indicated in the Figure Legends were transfected into cells after 48 hours of siRNA transfection.

Plasmids

The coding sequence of GC1 was amplified by PCR using the primers set (GC1_fw and GC1_rv) given in Table 1 and a KOD plus neo (TOYOBO) DNA polymerase with cDNA obtained from HEK293T cells as a template. The PCR product was subjected to agarose gel electrophoresis, recovered with the use of QIAEX II Gel Extraction Kit (QIAGEN), and subcloned into pCR-Blunt II-TOPO® vector involved in Zero Blunt® TOPO® PCR Cloning Kit (Thermo Fisher Scientific). Competent cells (strain JM109) were transformed with the resultant vector, incubated with super optimal broth with catabolite repression (SOC) medium for 1 hour at 37°C, and then cultured overnight on a Lysogeny broth (LB) agar plate containing 20 μg/ml kanamycin. The colonies grown were cultured in 2 ml of LB medium containing 20 μg/ml kanamycin and the plasmids were purified using FastGene Plasmid Mini Kit (NIPPON Genetics, Tokyo).

The coding sequence of GC1 was cleaved by the restriction enzymes *Xho*I and *Not*I, and was subcloned into the *Xho*I and *Not*I sites of pCAGGS-3×HA, pFX-SECFP, and pERedNLS-Flag-$Ca_v1.2$ (Fujioka et al., 2018), with the use of Rapid Ligation Kit (Roche), to obtain pCAGGS-3×HA-GC1, pFX-SECFP-GC1, pERedNLS-Flag-GC1, respectively. To generate the expression vector for eqFP650-, mKate2-, or MiCy-tagged GC1, the cording sequences of these fluorescent proteins were cleaved by *Eco*RI and *Bgl*II, and subcloned into the *Eco*RI and *Bgl*II sites of pFX-GC1-SECFP.

The coding sequences for helices 1-3 (1-127aa) and 4-6 (128-323aa) of GC1 were amplified by PCR with the primers listed in Table 1 and pFX-SECFP-GC1 as a template. The obtained PCR products were subcloned into the pCR-Blunt II-TOPO® vector, and were subjected to sequencing analysis, as described above. The coding sequences obtained were cleaved by *Xho*I and *Not*I, and ligated into the *Xho*I and *Not*I sites of pCAGGS-3×HA and pFX-eqFP650 to obtain pCAGGS-3×HA-1-3GC1, pCAGGS-3×HA-4-6GC1, pFX-eqFP650-1-3GC1, and pFX-eqFP650-4-6GC1.

pCAGGS-Venus-NT-H-Ras-WT, pCXN2-Flag-p110γRBD-Venus-CT (Tsutsumi et al., 2009), pCAGGS-CFP, pCAGGS-CFP-RAPEL, pCAGGS-GST, pCAGGS-GST-RAPEL (Fujioka et al., 2019), pFX-mito-MiCy and pFX-SECFP-TOM20 (unpublished data) were previously constructed in our laboratory. pDsRed-Mito were purchased from Clontech (Mountain View, CA, USA). pCMV-TagRFP-EEA-1 (42635) and pEX-PK-hLC3 (61458) were purchased from Addgene (Cambride, MA, USA). To construct an expression vector for a pH sensor targeted to the mitochondria, the coding sequence of a tandem heterodimer of fluorescent proteins, pH-sensitive pHluorin and pH-insensitive mKate2 was amplified by PCR with the primers listed in the Table 1 and with pEX-PK-hLC3 as a template. The obtained PCR products were subcloned into pCR-Blunt II-TOPO® vector. The coding sequences obtained were ligated into *Not*I and *Bgl*II sites of pFX-mito-MiCy. An ATP sensor based on the principle of Förster resonance energy transfer targeted to the mitochondria, mitoATeam 1.03 (Imamura et al., 2009) was a kind gift from Professor Hiroyuki Noji at the University of Tokyo. To construct pCXN2-Flag-GC1-IRES-SECFP, coding sequence of GC1 was out by *Xho*I and *Not*I from pCAGGS-3 × HA-GC1, and subcloned into the *Xho*I and *Not*I sites of pCXN2- Flag-p110γRBD-IRES-SECFP. Similarly, the control vector pCXN2-Flag-IRES-SECFP was prepared form pCXN2-Flag-GC1-IRES-SECFP by removing GC1 by digestion with *Xho*I and *Not*I, blunting with the Klenow enzyme, and self-ligation.

The sequences of PCR products that were subcloned into the pCR-Blunt II-TOPO® vector were confirmed by sequencing analyses with M13 forward and reverse primers, which were performed at the Institute for Genetic Medicine, Hokkaido University (Sapporo, Japan). The resulting sequences obtained were compared with the nucleotide sequences of GC1 (NM_001191060.1) obtained from the Nucleotide Database at the National Center for Biotechnology and Information (NCBI), with the use of DNA Dynamo software (Blue Tractor Software Ltd, Wales, UK).

Fluorescence microscopy and time-lapse imaging

Cells were visualized using the inverted research microscope IX-83 (Olympus, Tokyo, Japan) equipped with an sDISK spinning disk confocal module (Andor Technology Belfast, UK), a Biopoint MAC 6000 filter and shutter control unit (Lud1 Electronic Products, Hawthorne, NY, USA), a motorized XY stage (Chuo Precision Industrial, Tokyo, Japan), a cooled electron multiplying charge-coupled device (EMCCD) camera Rolera EM-C^2 (QImaging Surrey, BC, Canada), and the excitation light source SOLA Light Engine (Lumencor, Beaverton, OR, USA). The combinations of excitation and emission filters for each fluorescence used in this

study were: FF02-438/24 and FF01-483/32 (Semrock, Rochester, NY, USA) for cyan fluorescent protein (CFP); BP 470-490 and BP 510-550 (Olympus) for GFP and Alexa Fluor 488; FF 01-500/24-25 and FF 01-54/27 (Semrock) for yellow fluorescent protein (YFP); BP 520-550 and BA 580 IF (Olympus) for TagRFP, Alexa Fluor 546, and Alexa Fluor 594. A 60 × oil immersion objective with a numerical aperture of 1.35 or a 20 × objective with a numerical aperture of 0.75 (Olympus) were used. The surrounding environment of the sample was controlled using a Chamlide incubator system (Live cell instrument, Seoul, Korea). MetaMorph software (Universal Imaging, West Chester, PA, USA) was used to control the microscope and peripheral equipment.

Cells were seeded on type IC collagen-coated (Nitta Gelatin Inc., Osaka, Japan) 35 mm glass bottom dishes (Asahi Techno Glass, Sizuoka, Japan) at a density of 3.0×10^4. The cells were transfected with either siRNAs, expression vectors, or both, as indicated in the Figure Legends. Images were acquired every 1 minute for 70 minutes as mentioned in the Figure Legends. In some experiments, cells were serum starved in DMEM/F12 (Thermo Fisher Scientific) for 4 hours before time-lapse imaging. Ten minutes after time-lapse imaging had started, the cells were stimulated by EGF with a final concentration of 100 ng/ml.

Quantification of endosomal translocation of the Ras-PI3K complexes

From the background-subtracted images, vesicular structures that were positive for BiFC (Ras-PI3K complex) or TagRFP (EEA-1) were extracted using 'Top Hat' module of MetaMorph software. Colocalization area of the Ras-PI3K complex with EEA-1 was quantified with the use of 'Measure Colocalization' module of the software.

Measurement of mitochondrial pH, ATP concentration, and membrane potential

To determine pH in the mitochondria, the fluorescence intensities of pHlourin and mKate2 in the mitochondrial regions were quantified using MetaMorph software, and their ratio was calculated and plotted.

Cells expressing mitoATeam 1.03 were subjected to time-lapse imaging. After background subtraction, the fluorescence intensities in the mitochondrial region of CFP and FRET were used to calculate the emission ratio (FRET/CFP), which represents FRET efficiency and the ATP concentration in the mitochondria.

A431 cells transfected with either siRNAs against GC1 or control siRNA, or left untransfected, were seeded in a 35 mm glass bottom dish with the cell density of

approximately 3×10^4. The cells were then incubated with 250 nM TMRM at 37°C for 30 minutes. After washing three times with PBS, the cells were transferred into a phenol red-free DMEM/F12 medium and subjected to fluorescence microscopy. The fluorescence intensity of TMRM in the cells was quantified to evaluate mitochondrial membrane potential.

Mitochondrial morphology

To visualize the mitochondrial morphology, cells were treated with MitoTracker™ Red CMXRos at a final concentration of 12.5 nM for 10 minutes, washed three times with PBS, and cultured in a phenol red-free DMEM/F12 medium. Mitochondrial fragmentation was assessed using ImageJ software (https://imaegj.nih.gov/ij) as described previously (Giedt et al., 2016; Rahman et al., 2012). Briefly, the median filter was applied to an original image, from which the background signal had been subtracted, and the resulting image was converted into an 8-bit image. Next, a binarized image was created using the 'Auto Local Threshold' of ImageJ Plugin to extract the mitochondrial regions. The binarized image was subjected to morphology filters (opened and then closed) to remove noise. With this mitochondrial mask image, the number of mitochondria (particles) and the area of each mitochondrion were measured using the 'Particle Counting' Plugin of ImageJ. The number of mitochondria × 10,000 / total area of mitochondria (pixel) was calculated and plotted, which is considered to reflect an extent of mitochondrial fragmentation.

Evaluation of endosome acidification

HeLa or A431 cells transfected with expression plasmids were incubated with Alexa Fluor 488-labeled dextran and AcidiFluor™ ORANGE-labeled dextran (final concentration: 500 μg/ml and 200 μg/ml, respectively), or 10 nM LysoTracker Red at 37°C for 15 minutes. Cells were washed three times with ice-cold PBS and transferred into the phenol red free DMEM/F12 medium. Images obtained were subjected to background subtraction. To determine endosome acidification by AcidiFluor™ ORANGE-labeled dextran, fluorescence intensities of Alexa Fluor 488 and AcidiFluor™ ORANGE were quantified and their ratio was calculated and plotted. Note that AcidiFluor™ ORANGE-labeled dextran is pH sensitive, whereas Alexa Fluor 488-labeled dextran is insensitive. To determine endosome acidification by LysoTracker Red, fluorescence intensities of LysoTracker Red in the cells were quantified and plotted.

Dextran and transferrin uptake

A431 cells transfected with expression plasmids were incubated with fluorescently labeled dextran or transferrin (Alexa Fluor 488 or Alexa Fluor 546) at a final concentration of 500 μg/ml for 10 minutes or 30 minutes at 37°C. The cells were washed three times with ice-cold PBS, followed by treatment with trypan blue for 30 seconds to quench cell surface dextran. Images obtained were subjected to background subtraction and quantification of fluorescence intensities, so that the uptake of dextran and transferrin could be evaluated.

Immunofluorescence

Cells were washed with PBS, fixed with 3% paraformaldehyde for 15 minutes at room temperature, and permeabilized with 0.1% Triton X-100 in PBS for 4 minutes at room temperature. After washing with PBT (PBS containing 0.1% bovine serum albumin (BSA) and 0.05% Triton X-100), the cells were then incubated with 1% BSA for 30 minutes at room temperature to block nonspecific binding of antibodies. The cells were further incubated with primary antibodies (GC1, 1:1,000; HA, 1:1,000; FLAG, 1:1,000) overnight at 4°C. The cells were then incubated with Alexa Fluor 488, Alexa Fluor 594, or Alexa Fluor 647-conjugated secondary antibodies (1: 250) for 1 hour at room temperature. After washing with PBT and PBS, cells were observed with the above-mentioned imaging workstation or an Olympus confocal laser microscope FV10i.

Statistical analysis method

All data are shown as the mean ± s.e.m. from at least three independent experiments (unless indicated otherwise) and were compared by Student's *t*-test (between two conditions) or one-way analysis of variance (ANOVA) followed by Dunnett's post-hoc analysis (among multiple conditions). Time series data sets were compared by multivariate analysis of variance (MANOVA) (between two conditions) or MANOVA with Bonferroni correction (among multiple conditions).

Table 1. Primers used in this study

Primer Name	Sequence (5′ to 3 ′ direction)
GC1-F	GGCTCGAGATGGCTGATAAGCAGATCAGCCTG
GC1-R	GGGCGGCCGCAGGCCTGGGGGTCCTGCAG
GC1-qPCR-F	TACACGGGCATGTCCGACTG
GC1-qPCR-R	CAGCTTCTGCCCGTCCTTAG
GAPDH-F	AATCCCATCACCATCTTCCA
GAPDH-R	TGGACTCCACGACGTACTCA
GC1-TM-1-3-F	GGCTCGAGATGGCTGATAAGCAGATCAGCCTG
GC1-TM-1-3-R	GGGCGGCCGCATGCATCCTGCAGCTGGATCTT
GC1-TM-4-6-F	GGCTCGAGGGCACCATGAAGATCCAGCTGCAGGATGCA
GC1-TM-4-6-R	GGGCGGCCGCAGGCCTGGGGGTCCTGCAG
pHluorin-F	GGGCGGCCGCATGAGTAAAGGAGAAGAACTTTTCA
mKate2-R	GGAGATCTTCTGAGTCCGGAACCTCCTC

RESULTS

Mitochondrial membrane protein GC1 interacts with RAPEL

From our laboratory, it was previously reported that in the presence of EGF, the Ras-PI3K complexes specifically translocate from the plasma membrane to endosomes and Ras-PI3K signaling from the endosome promotes clathrin-independent endocytosis and endosomal maturation (Fujioka et al., 2011; Tsutsumi et al., 2009). However, the precise molecular mechanism through which Ras-PI3K complexes are localized in the endosome is still unknown. Our laboratory has identified the 28-amino acid sequence that is specifically found in RBD of PI3K, but not in those of other effector molecules, and revealed that this peptide is involved in the translocation of Ras-PI3K complex to the endosome (Fujioka et al., 2019). The peptide was named RAPEL after Ras-PI3K endosomal localization. Through screening of RAPEL-binding factors with the use of yeast two-hybrid system and immunoprecipitation followed by mass spectrometry, 48 potential binding proteins to RAPEL have been isolated (manuscripts in preparation). Among these factors, I focused on glutamate carrier protein-1 (GC1), a mitochondrial membrane protein that is involved in the transport of glutamate along with H^+ (Palmieri, 2014).

First, I tested whether GC1 biochemically interacts with RAPEL. HEK293T cells were transfected with expression vectors for HA-tagged GC1 and ECFP-tagged RAPEL, and cell lysates collected from the cells were subjected to immunoprecipitation with an anti-GFP (which can also recognize ECFP) antibody and protein G Sepharose beads, followed by immunoblot analysis. As shown in **Figure 1A**, the GC1 protein could be detected in the anti-GFP immunoprecipitates only in the presence of both GC1 and RAPEL (top panel, lane 4). Next, immunoprecipitation of the same sample was also performed with the use of an anti-HA antibody and essentially similar result was obtained (**Figure 1B**), demonstrating the interaction of GC1 with RAPEL. The interaction between endogenous GC1 and exogenous RAPEL was also confirmed (**Figure 1C**). I further investigated whether GC1 interacts with full-length PI3K and found that GC1 interacts with full-length PI3K irrespective of the presence or absence of EGF (**Figure 1D**). Taken together, these results demonstrated that GC1 indeed binds to RAPEL in the RBD of PI3K in an EGF-independent manner.

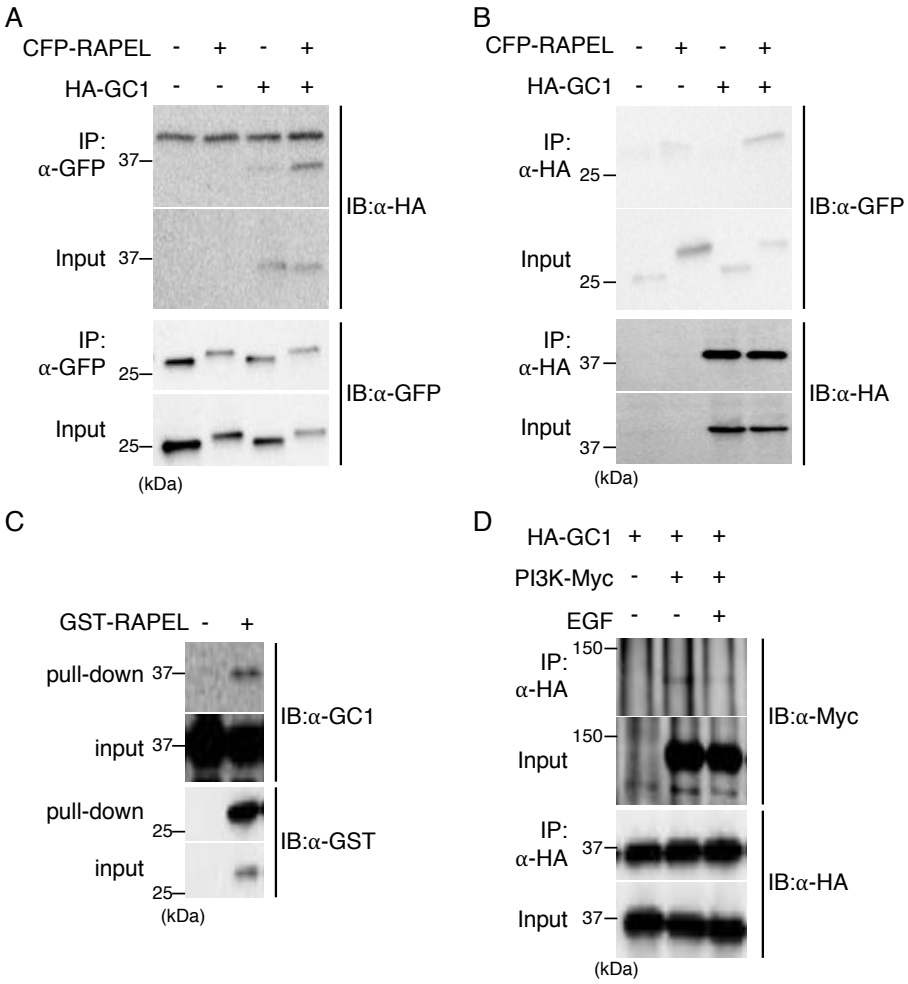

Figure 1. GC1 interacted with RAPEL

(A and B) HEK 293T cells were transfected with the expression vectors encoding HA-GC1 and ECFP-RAPEL as indicated. Total cell lysates (TCL) were incubated with anti-GFP (A) or anti-HA (B) antibodies, and protein G Sepharose beads. Immunoprecipitates and aliquots of cell lysates were subjected to SDS-PAGE, and separated proteins were analyzed by immunoblotting with the use of anti-HA and anti-GFP antibodies. Images shown are the representative from three independent experiments.

(C) TCL prepared from HEK293T cells expressing GST-RAPEL were subjected to pull-down assay with glutathione Sepharose beads followed by immunoblot analysis with the use of anti-GST and anti-HA antibodies.

(D) HEK293T cells were transfected with the expressing vectors for HA-GC1 and PI3K-Myc as indicated. The cells were serum-starved for 4 hours and stimulated by EGF for 15 minutes. TCL extracted from the cells were subjected to immunoprecipitation with anti-HA antibody, followed by immunoblot analysis using anti-HA and anti-Myc antibodies.

GC1 is localized in the mitochondria

I next examined the intracellular localization of GC1. Because it has been reported that GC1 is localized in the mitochondria (Casimir et al., 2009), I first assessed whether GC1 is indeed localized in this organelle. Cos-1 cells were transfected with expression vectors for HA-GC1 and mito-SECFP, a marker of the mitochondrial matrix, and subjected to immunofluorescence with the use of an anti-HA antibody. Confocal microscopic observation demonstrated that HA-GC1 was colocalized with mito-SECFP (**Figure 2A**). To further support this result, I examined the localization of endogenous GC1 with the use of an anti-GC1 antibody and found that it was also colocalized with both mito-SECFP and SECFP-TOM20, a marker for the mitochondrial outer membrane (**Figures 2B** and **2C**). These results together indicated that GC1 is localized in the mitochondria.

Because fluorescent proteins are powerful tools to visualize molecular dynamics in living cells (Day and Schaufele, 2008), fluorescent protein-tagged GC1 was therefore prepared. However, in living Cos-1 cells, fluorescence microscopic analysis unexpectedly revealed that SECFP-GC1 was localized diffusely in the cytoplasm (**Figure 3A**), suggesting that the fast folding of tagged SECFP caused mislocalization of mitochondrial proteins (manuscript in preparation). Therefore, I constructed expression vectors for GC1 tagged with either MiCy, mKate2, or near-infrared fluorescent protein eqFP650, whose folding rate is slower than that of SECFP (Balleza et al., 2018). MiCy-tagged GC1 was localized not only in the mitochondria but also in the cytosol (**Figure 3B**), whereas GC1-mKate2 and eqFP-GC1 were preferentially localized in mitochondria (**Figures 3C and 3D**). According to these results, GC1-mKate2 was used in the following experiments.

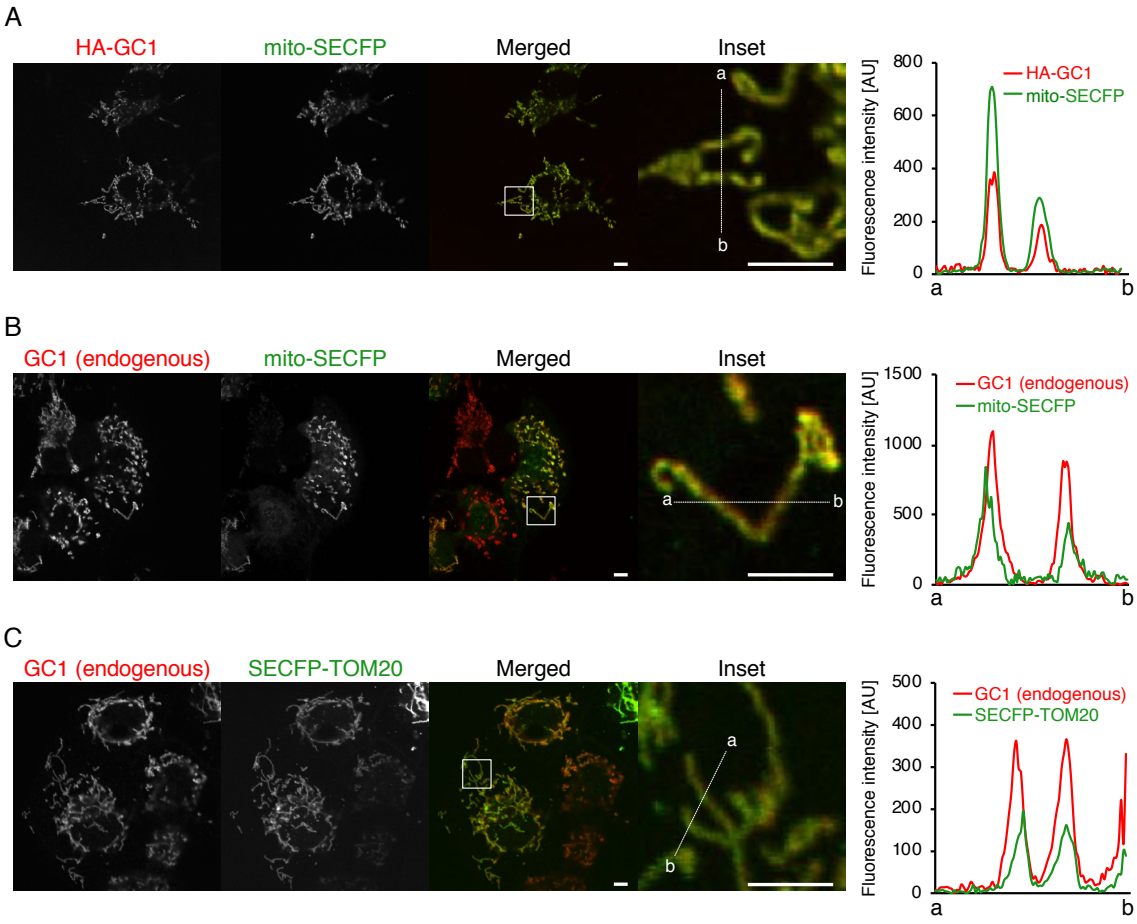

Figure 2. GC1 was localized in mitochondria

(**A**–**C**) Cos-1 cells were transfected with expression vectors for HA-GC1 and mito-SECFP (**A**), that for mito-SECFP (**B**), or that for SECFP-TOM20 (**C**). Twenty-four hours after transfection, the cells were fixed and then subjected to an immunofluorescence with the use of an anti-HA (**A**) or anti-GC1 (**B** and **C**) antibody, and further incubated with an Alexa Fluor 594-conjugated secondary antibody. Representative confocal images are shown. Bars, 10 μm. Fluorescence intensities of GC1 (red) and mitochondria (green) along with the line in the merged images were plotted from a to b. Images shown are the representative from three independent experiments.

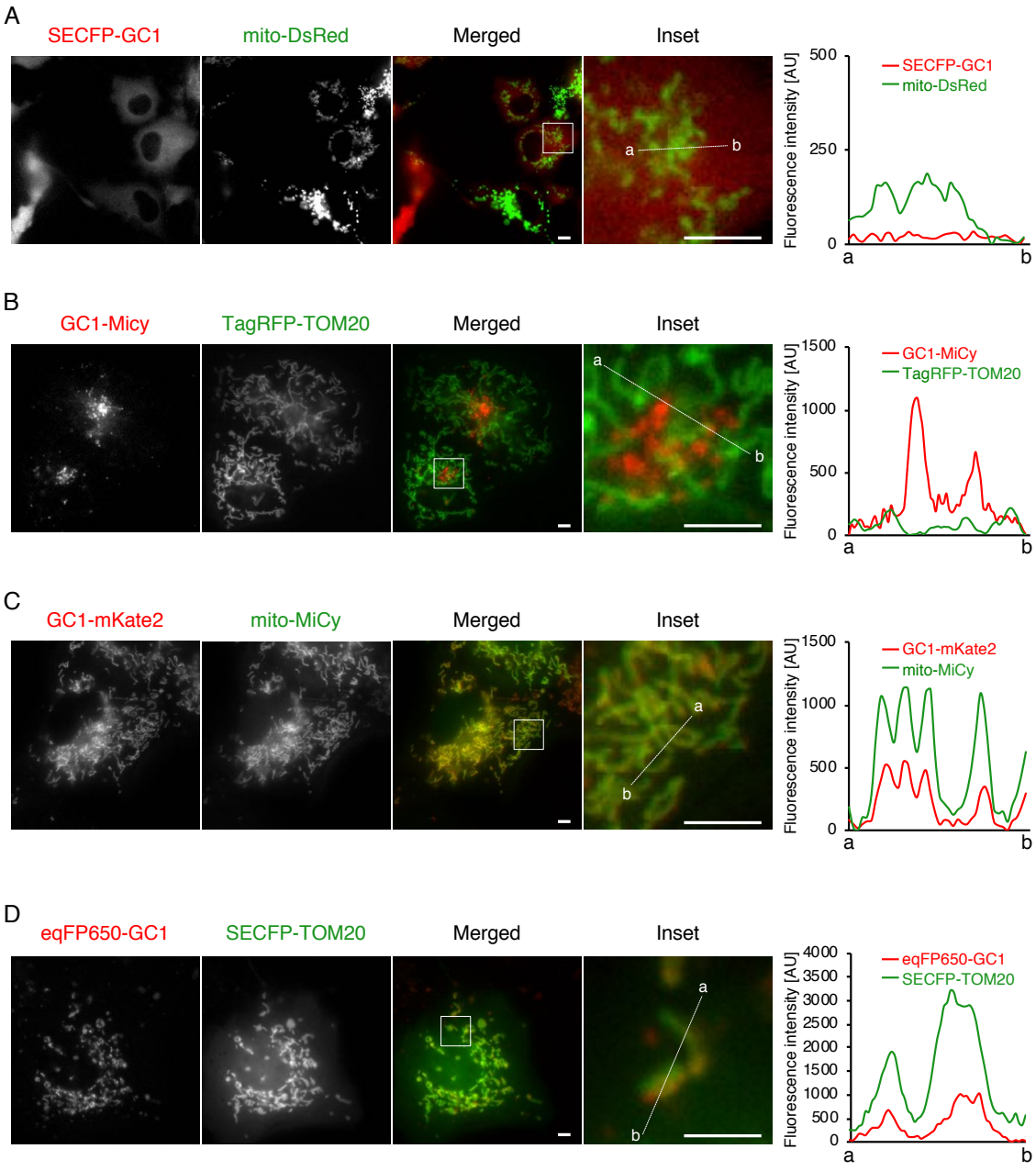

Figure 3. mKate2 tagged GC1 was preferentially localized in mitochondria

(**A**–**D**) Cos-1 cells were transfected with expression vectors for SECFP-GC1 and mito-DsRed (**A**), GC1-MiCy and TagRFP-TOM20 (**B**), GC1-mKate2 and mito-MiCy (**C**), or eqFP650-GC1 and SECFP-TOM20 (**D**). Twenty-four hours after transfection, the cells were subjected to fluorescence microscopy. Representative images are shown. Bars, 10 μm. Fluorescence intensities of GC1 (red) and mitochondria (green) along with the line in the merged images were plotted from a to b.

GC1-positive mitochondria are localized in close proximity with Ras-PI3K complex-positive endosomes

Although GC1 was confirmed to be localized in the mitochondria, it is unclear how the mitochondrial GC1 interacts with Ras-PI3K complexes in the endosome (or at the plasma membrane) through RAPEL. To clarify this notion, I performed live-cell confocal imaging of Ras-PI3K complexes, early endosome, and GC1, which were visualized by the BiFC method (Tsutsumi et al., 2009), the early endosome marker EEA-1 tagged with SECFP, and GC1-mKate2, respectively (**Figure 4A**). Line scan analysis revealed that Ras-PI3K complex-positive endosomes were localized in close proximity with GC1-positive mitochondria (**Figure 4B**). This result might further indicate the possibility that endosomes interacts with mitochondria through binding between GC1 and Ras-PI3K complex.

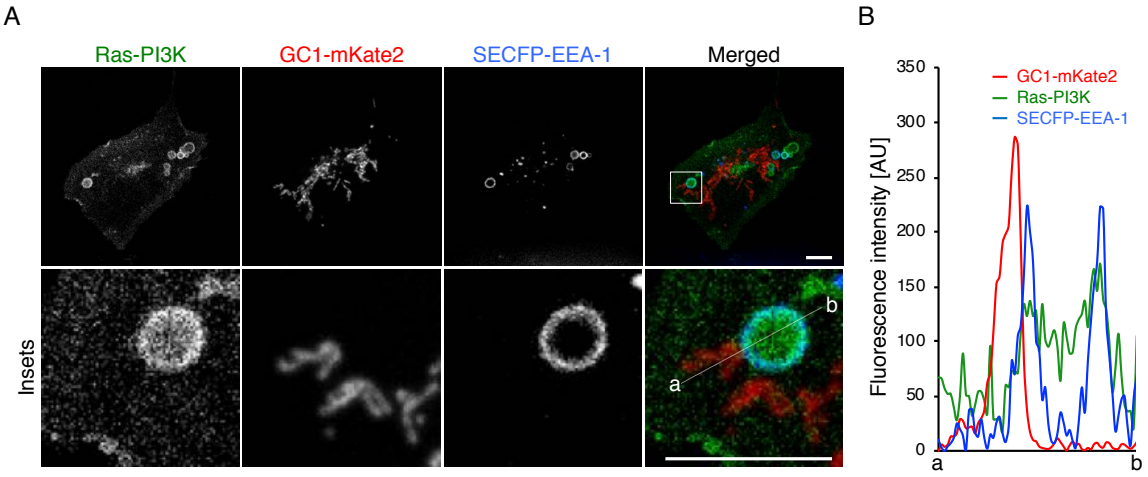

Figure 4. GC1 was localized in close proximity to the endosomes in which the Ras-PI3K complexes resided

(**A**) A431 cells were transfected with expression vectors for GC1-mKate2, VN-H-Ras, p110 γ RBD-VC, and SECFP-EEA-1. After serum starvation for 4 hours, the cells were subjected to time-lapse confocal microscopy. Starting at 10 minutes, the cells were exposed to EGF. Representative images were shown. Bars, 10 μ m. Images shown are the representative from three independent experiments.

(**B**) Fluorescence intensities of GC1 (red), Ras-PI3K (green), and EEA-1 (blue) along with the line in the merged images were plotted from a to b.

GC1 is localized in both the inner and outer membrane of mitochondria.

To interact with cytosolic or endosomal PI3K, GC1 should be localized in the mitochondrial outer membrane. However, as far as I am aware, there is only one report for the localization of GC1, in which GC1 is regarded as an inner mitochondrial membrane protein (Casimir et al., 2009). To determine the precise localization of GC1 into my own hands, I utilized the mega-mitochondria method using valinomycin (Heidler et al., 2011). Valinomycin is a potassium ionophore, which induces potassium influx from the cytosol into mitochondria, resulting in mitochondrial swelling (mega-mitochondria). The inner and outer membranes of mitochondria are thereby distinguished by confocal microscopy. In fact, in the absence valinomycin, localization of the outer membranate marker SECFP-TOM20 and the matrix marker mito-MiCy could not be distinguished from each other (**Figure 5A**), while they displayed distinct localization (**Figure 5B**) in the presence of this reagent. Under this condition, the localization pattern of GC1 was rather similar to that of TOM20 than that of mito (**Figures 5C** and **5D**). This result indicated that GC1 is localized not only in the inner membrane, but also in the outer membrane of mitochondria.

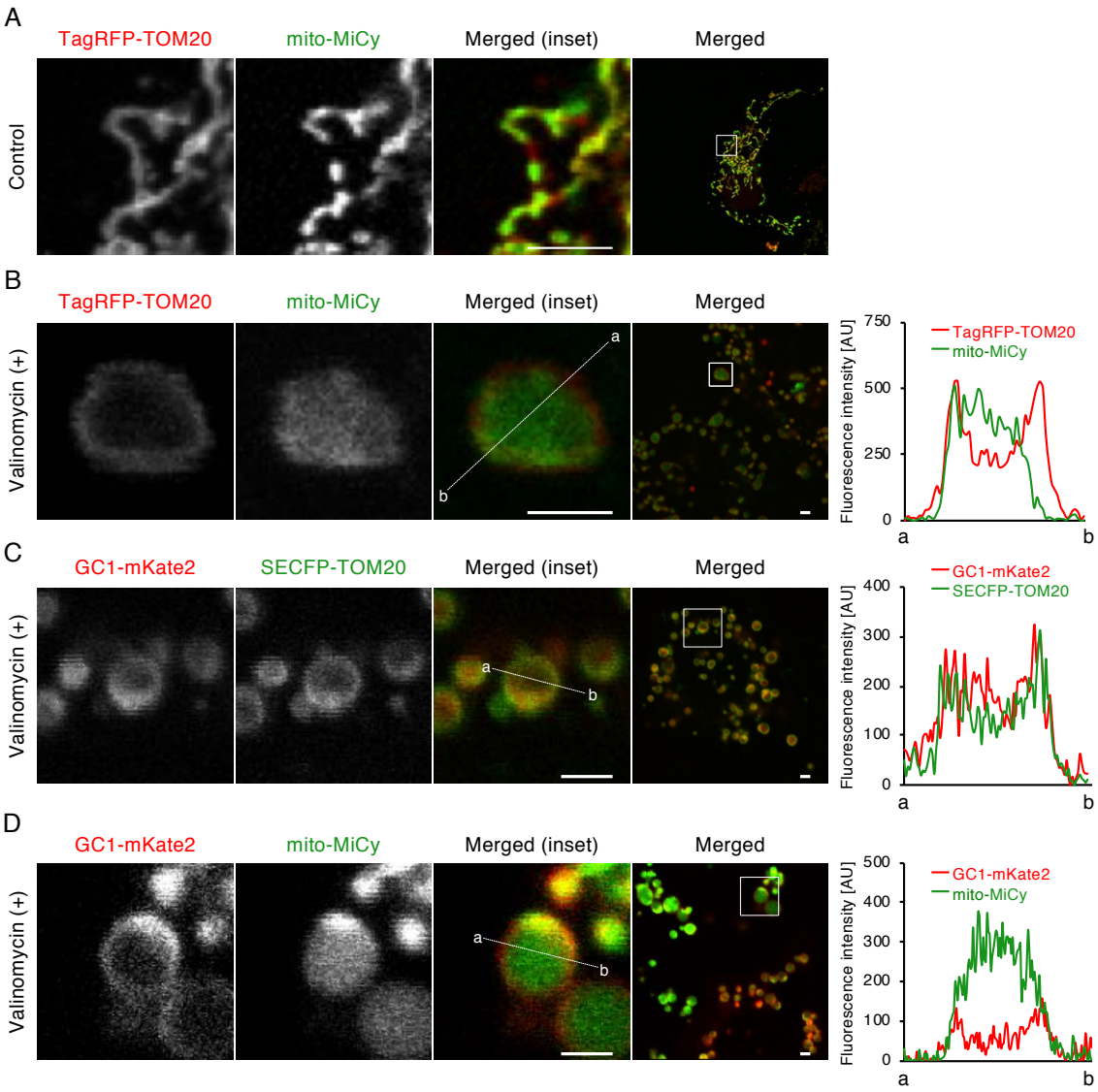

Figure 5. GC1 was localized in both the inner and outer membrane of mitochondria

(**A**–**D**) Cos-1 cells expressing TagRFP-TOM20 and mito-MiCy (**A** and **B**), GC1-mKate2 and SECFP-TOM20 (**C**), or GC1-mKate2 and mito-MiCy (**D**) were treated with (**B**–**D**) valinomycin for 10 minutes or left untreated (**A**). Representative confocal images are shown. Bars, 10 μ m. Fluorescence intensities along with the line in the merged images were plotted from a to b.

N-terminus and C-terminus of GC1 are respectively responsible for its interaction with RAPEL and mitochondrial localization

GC1 consists of six alpha helices that traverse the mitochondrial membrane, and helices 2 and 3 are required for its function as a glutamate transporter (Frigerio et al., 2008). Next, in order to identify the region responsible for GC1 binding to RAPEL, I prepared the expression vectors for two truncation mutants of GC1, GC1_1-127 and GC1_128-323 which consist of 1–127 (1–3 helices) and 128–323 (4–6 helices) amino acids, respectively, or full-length GC1, each tagged with eqFP650 (**Figure 6A**). Total cell lysates from cells expressing eqFP650-tagged GC1 and GST-tagged RAPEL were subjected to pull-down assay. It was revealed that full-length GC1 and GC1_1-127, but not GC1_128-323, interacted with RAPEL (**Figure 6B**). Next, I examined the localization of the truncation mutants of GC1. For this, expression vectors for HA-tagged GC1 truncation mutants were prepared, and Cos-1 cells transfected with such vectors were subjected to immunofluorescence with an anti-HA antibody. Confocal microscopic observation revealed that full-length GC1 and GC1_128-323 were colocalized with mito-MiCy, whereas GC1_1-127 was localized diffusely in the cytoplasm (**Figure 6C**). Taken together, these results suggested that N-terminal and C-terminus regions of GC1 are crucial for mitochondrial localization and interaction with RAPEL, respectively.

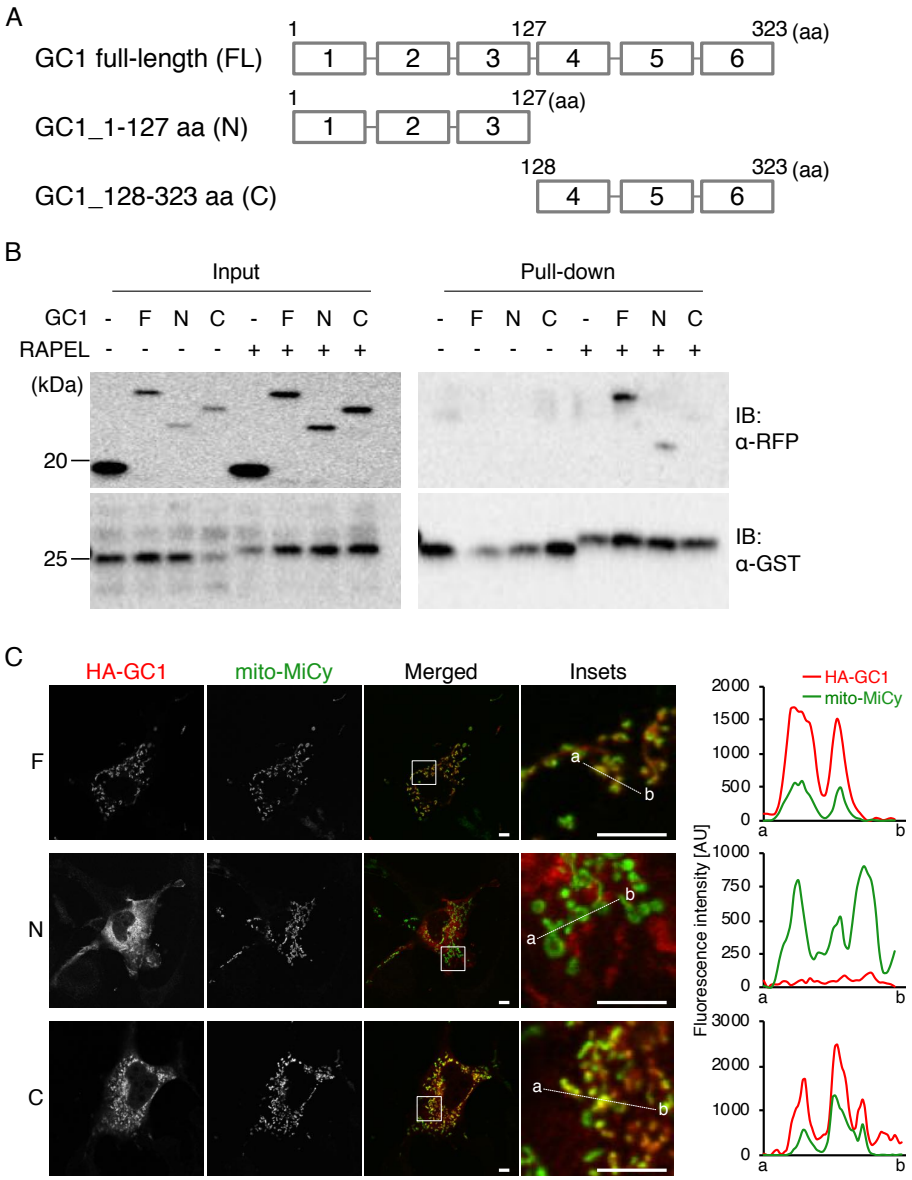

Figure 6. N-terminus and C-terminus of GC1 were responsible for its interaction with RAPEL and mitochondrial localization, respectively

(**A**) Schematic diagram for full length and truncation mutants of GC1.

(**B**) TCL from HEK293T cells expressing eqFP650-GC1 and GST-RAPEL were subjected to pull-down assay followed by immunoblot analysis with the use of anti-RFP and anti-GST antibodies.

(**C**) Cos-1 cells expressing HA-tagged full-length GC1 or its truncation mutants with mito-MiCy were fixed, and subjected to immunofluorescence with the use of an anti-HA antibody. Representative confocal images are shown. Bars, 10 μm. Fluorescence intensities of GC1 (red) and mitochondria (green) along with the line in the merged images were plotted from a to b.

GC1 negatively regulates endosome localization of Ras-PI3K complex

Next, I examined whether GC1 is involved in the regulation of endosomal localization of Ras-PI3K complexes. For this purpose, I performed BiFC imaging in GC1-knockdown cells. When siRNAs against GC1 (siGC1 #5 and siGC1 #7) were transfected into A431 cells, mRNA levels and protein levels of GC1 were reduced up to 85%, as revealed by qPCR analysis (**Figure 7A**) and immunoblotting (**Figure 7B**), respectively. Under this condition, the extent of the endosome localization of Ras-PI3K complexes, which was determined by colocalization of signals of Ras-PI3K complex and EEA-1, was increased upon EGF stimulation (**Figures 7C** and **7D**), as reported previously (Fujioka et al., 2019), and in GC1 knocked down cells, it was significantly accelerated (**Figure 7C** and **7D**). These results indicated that GC1 negatively regulates the endosomal localization of Ras-PI3K complexes.

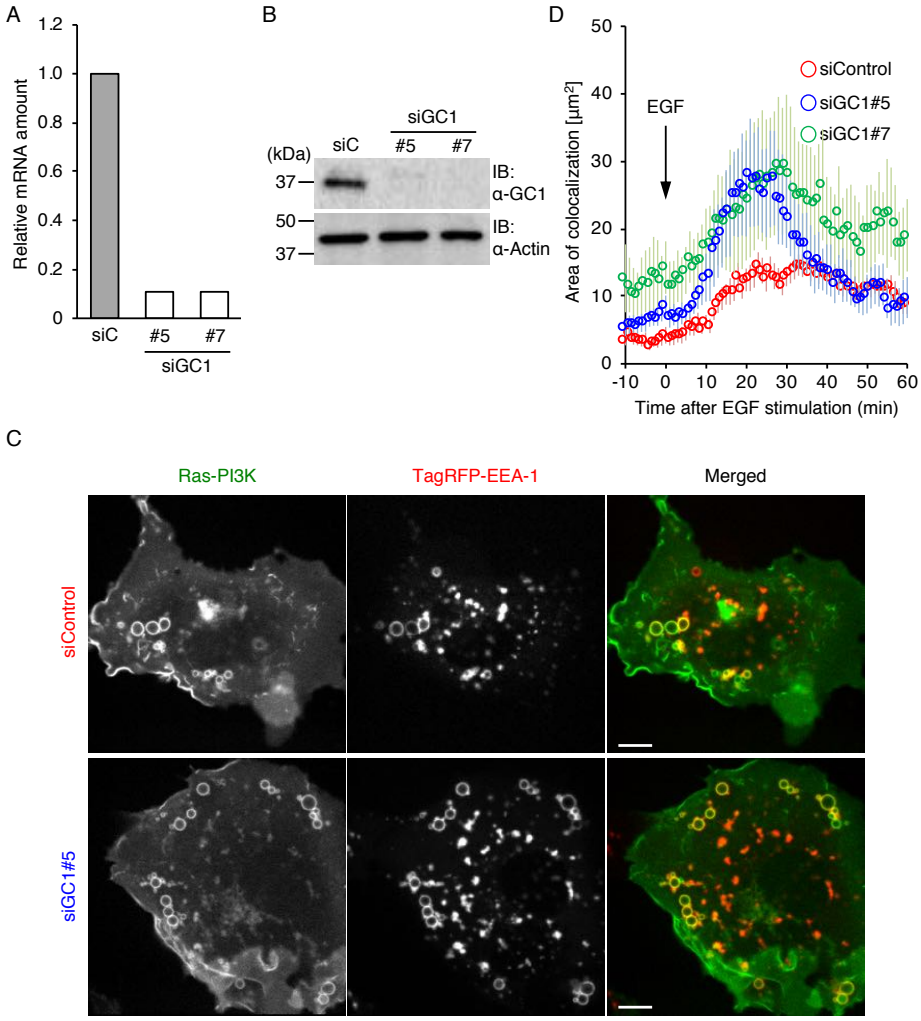

Figure 7. Knockdown of GC1 promoted the translocation of Ras-PI3K complexes to endosomes

(**A**) A431 cells were transfected with either control siRNA (siC) or siRNA against GC1 (siGC1 #5 and #7) for 48 hours. Total RNA isolated from the cells was subjected to reverse transcription (RT) and quantitative polymerase chain reaction (PCR) analysis. mRNA expression levels of GC1 were normalized by that of GAPDH and plotted.

(**B**) A431 cells were transfected with either siC or siGC1 for 72 hours. TCL extracted from the cells were subjected to immunoblot analysis with the use of anti-GC1 and anti- β -actin antibodies.

(**C** and **D**) A431 cells transfected with either siC or siGC1 for 48 hours were further transfected with the expression vectors for TagRFP-EEA-1, VN-H-RasWT, and p110 γ RBD-VC for 24 hours. The cells were serum starved for 4 hours and subjected to time-lapse confocal microscopy. Representative images at 30 minutes after EGF stimulation are shown (**C**). Bars, 10 μ m. The extent of colocalization of the EEA-1 and Ras-PI3K complexes was quantified and plotted (**D**). Data are presented as the mean ± s.e.m. ($n \geq 10$ from three independent experiments). $P < 0.0001$ as calculated by MANOVA.

GC1 negatively regulates clathrin-independent endocytosis

Previous research in our laboratory demonstrated that Ras-PI3K signaling is involved in clathrin-independent endocytosis and endosomal maturation (Fujioka et al., 2011). I therefore investigated whether GC1 is involved in the regulation of clathrin-independent endocytosis with the use of fluorescently labeled 10-kDa dextran, which is known to be internalized into cells via a clathrin-independent endocytosis pathway, was evaluated. Exogenous expression of FLAG-tagged GC1 suppressed dextran uptake by approximately 25%, as compared to that in control cells (**Figure 8A**). Expression of mKate2-tagged GC1 also suppressed the dextran uptake (**Figure 8B**). To further confirm the role of GC1 in the regulation of clathrin-independent endocytosis, I performed knockdown experiments. For this, in addition to siGC1 #5 and siGC1 #7, siGC1 #1 targeted to the 3′ UTR region of GC1 mRNA was recruited, aiming at performing rescue experiments thereafter. The knockdown efficacy of siGC1 #1 was similar to those of siGC #5 and #7, as confirmed by immunoblotting analysis (**Figure 9A**). The uptake of dextran was significantly upregulated in GC1-knockdown cells (**Figure 9B**).

To provide more evidence for these findings, I performed rescue experiments, in which wild-type GC1 was re-introduced into A431 cells that had been depleted of endogenous GC1 by siGC1 #1. A431 cells transfected with control siRNA or siGC1 #1 for 48 hours, were further transfected with expression vectors for GC1. Twenty-four hours after transfection, the cells were incubated with fluorescently labeled dextran. Microscopic observation revealed that exogenous expression of GC1 in GC1 knockdown cells counteracted the increase in fluorescence intensity of dextran (**Figure 10**). These results together demonstrated that GC1 is a negative regulator for clathrin-independent endocytosis.

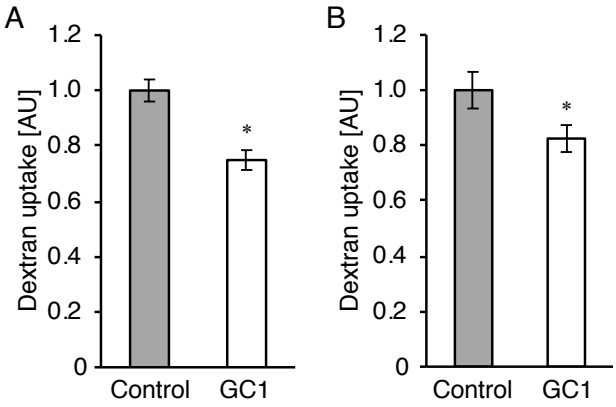

Figure 8. Overexpression of GC1 inhibited clathrin-independent endocytosis

(**A** and **B**) A431 cells were transfected with an expression vector encoding FLAG-GC1 (**A**) or GC1-mKate2 (**B**). Twenty-four hours after transfection, the cells were incubated with Alexa Fluor 546-labeled dextran for 10 minutes at 37°C, washed with PBS, and then treated with trypan blue. Total fluorescence intensities within the cells were quantified and plotted. Data are presented as the mean ± s.e.m. ($n \geq 90$ from three independent experiments). *$P < 0.05$ versus control vector-transfected cells, as calculated by Student's *t*-test.

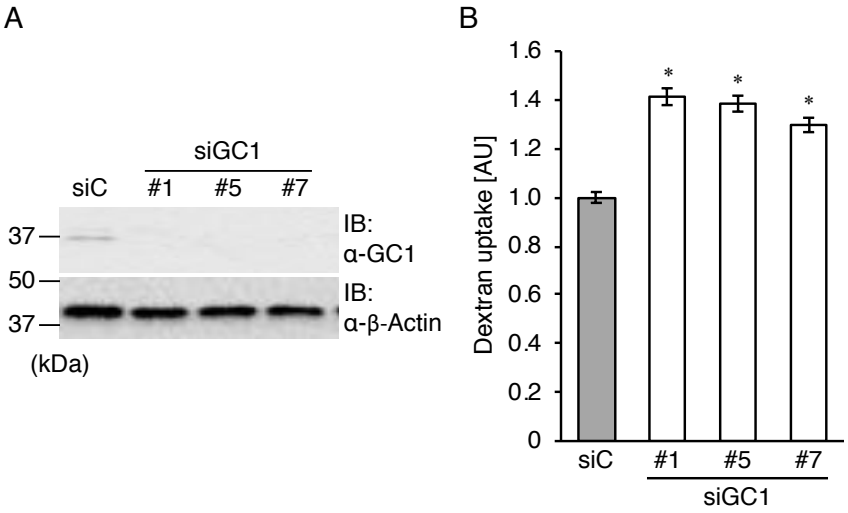

Figure 9. GC1 knockdown enhanced clathrin-independent endocytosis

(**A**) A431 cells were transfected with either siC or siGC1 for 72 hours. TCL were collected and subjected to immunoblotting analysis with anti-GC1 and anti- β -actin antibodies.

(**B**) A431 cells were transfected with either siC or siGC1 for 72 hours. The cells were incubated with Alexa Fluor 546-labeled dextran for 10 minutes at 37°C. Total fluorescence intensities within the cells were quantified and plotted. Data are presented as the mean ± s.e.m. ($n \geq 470$ from three independent experiments). *$P < 0.0001$ versus siC-transfected cells, as calculated by one-way ANOVA with Dunnett's post-test.

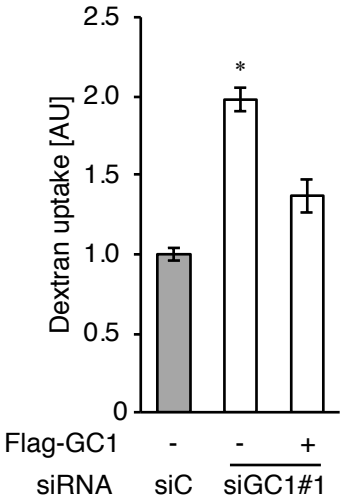

Figure 10. Exogenously expression of GC1 cancelled promotion of clathrin-independent endocytosis in GC1-knockdown cells

A431 cells were first transfected with either siC or siGC#1 for 48 hours and were further transfected with expression vectors for FLAG-GC1. The cells were incubated with Alexa Fluor 546-labeled dextran for 10 minutes at 37°C. Total fluorescence intensities within the cells were quantified and plotted. Data are presented as the mean ± s.e.m. ($n \geq 70$ from three independent experiments). *$P <$ 0.05 versus siC-transfected cells, as calculated by one-way ANOVA with Dunnett's post-test.

GC1 positively regulates clathrin-dependent endocytosis

Next, the role of GC1 in the regulation of clathrin-dependent endocytosis was examined by quantifying the uptake of transferrin, which is incorporated into cells through clathrin-dependent endocytosis. In GC1-overexpressing A431 cells, fluorescence intensities of transferrin were increased (**Figure 11A** and **11B**), whereas it was decreased in GC1-knockdown cells (**Figure 11C**). Thus, in contrast to clathrin-independent endocytosis, clathrin-dependent endocytosis might be positively regulated by GC1.

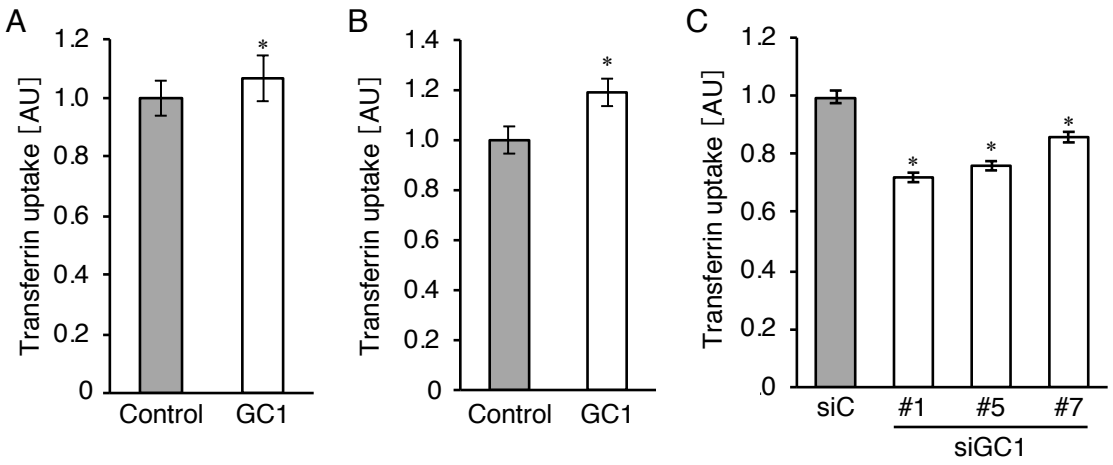

Figure 11. GC1 positively regulates clathrin-dependent endocytosis

(**A** and **B**) A431 cells were transfected with an expression vector encoding FLAG-GC1 (**A**) or GC1-mKate2 (**B**). Twenty-four hours after transfection, the cells were incubated with Alexa Fluor 546-labeled transferrin for 30 minutes at 37°C, washed with PBS, and then treated with trypan blue. Total fluorescence intensities within the cells were quantified and plotted. Data are presented as the mean ± s.e.m. ($n \geq 75$ from three independent experiments). *$P < 0.05$ versus control vector-transfected cells, as calculated by Student's *t*-test.

(**C**) A431 cells were transfected with either siC or siGC1 for 72 hours. The cells were incubated with Alexa Fluor 546-labeled transferrin for 30 minutes at 37°C. Total fluorescence intensities within cells were quantified and plotted. Data are presented as the mean ± s.e.m. ($n \geq 330$ from three independent experiments). *$P < 0.0001$ versus siC-transfected cells, as calculated by one-way ANOVA with Dunnett's post-test.

GC1 negatively regulates endosomal maturation

Next, to examine the role of GC1 in the regulation of endosomal maturation, cells expressing HA-GC1 were incubated with LysoTracker Red, a red fluorescent dye for labeling acidic organelles in living cells, and subjected to fluorescence microscopy. The total fluorescence intensity was decreased in HA-GC1-expressing A431 cells (**Figure 12A**) and HeLa cells (**Figure 12B**), indicating that the acidity and/or the number of lysosomes is decreased by GC1 expression. To further support this finding, similar experiments were performed with the use of the pH-sensitive fluorescent dye AcidiFluor™ ORANGE-labeled dextran, which is incorporated into cells via endocytosis and the fluorescence intensity is increased under acidic condition. Because overexpression of GC1 inhibits dextran uptake (**Figures 8A** and **8B**), the

fluorescence intensity of AcidiFluor™ ORANGE-labeled dextran was divided by that of pH-insensitive Alexa Fluor 488-labeled dextran (as a reference), to normalize the difference in the amount of dextrans. The ratio (AcidiFluor™ ORANGE/Alexa Fluor 488) in HA-GC1-expressing cells was lower than that in control cells (**Figure 12C**).

Next, the effect of GC1 knockdown on endosome maturation was evaluated. Total fluorescence intensity of LysoTracker in GC1-knockdown cells was higher than that in control cells (**Figure 13A**). In addition, reintroduction of GC1 in GC1-knockdown cells cancelled the increased fluorescence intensity of LysoTracker (**Figure 13B**). These results confirmed that GC1 negatively regulates endosomal maturation.

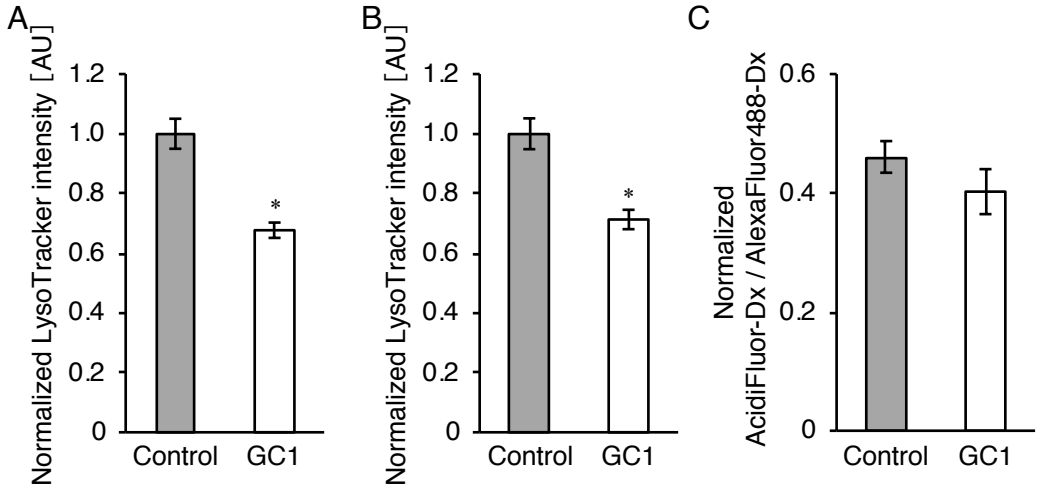

Figure 12. Overexpression of GC1 suppressed endosomal maturation

(**A** and **B**). A431 (**A**) or HeLa (**B**) cells were transfected with a control vector or an expression vector for HA-GC1. The cells were incubated with LysoTracker Red for 15 minutes at 37°C and subjected to fluorescence microscopy. Total fluorescence intensities within the cells were quantitated and plotted. Data are presented as the mean ± s.e.m. ($n \geq 160$ (**A**) or $n \geq 80$ (**B**) from three independent experiments). *$P < 0.001$ versus control vector-transfected cells, as calculated by Student's *t*-test.

(**C**) HeLa cells expressing HA-GC1 were incubated with Alexa Fluor 488-labeled dextran (AlexaFluor488-Dx) and AcidiFluor™ ORANGE-labeled dextran (AcidiFluor-Dx) for 15 minutes. The cells were washed with PBS and then subjected to fluorescence microscopy. The ratio of fluorescence intensities of AcidiFluor-Dx and Alexa Fluor 488-Dx was calculated and plotted. Data are presented as the mean ± S.D. ($n \geq 20$ from one experiment).

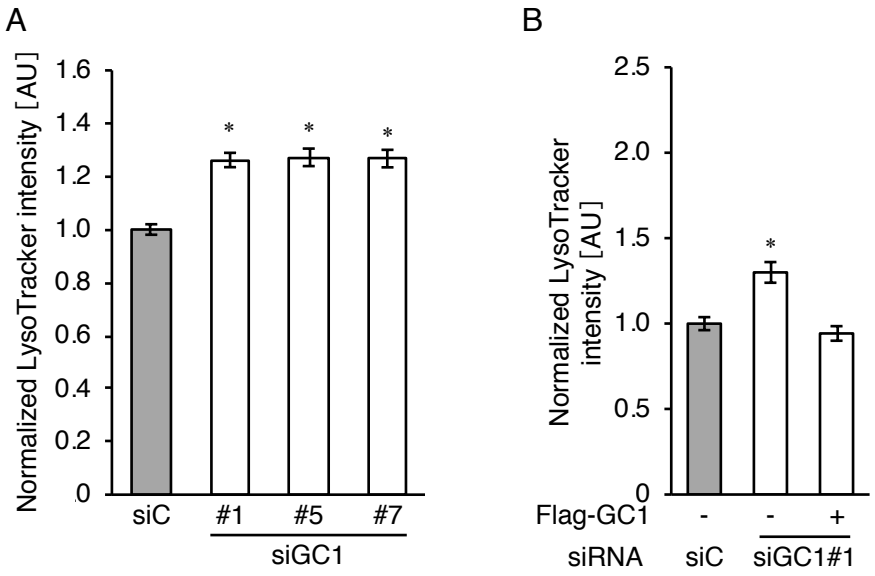

Figure 13. GC1 negatively regulates endosome maturation

(**A**) A431 cells were transfected with either siC or siGC1 for 72 hours. The cells were incubated with LysoTracker Red for 15 minutes at 37°C. Total fluorescence intensities within the cells were quantified and plotted. Data are presented as the mean ± s.e.m. ($n \geq 295$ from three independent experiments).

(**B**) A431 cells were first transfected with either siC or siGC#1 for 48 hours, and were further transfected with an expression vectors for FLAG-GC1. The cells were incubated with LysoTracker Red for 15 minutes at 37°C. Total fluorescence intensities within the cells were quantified and plotted. Data are presented as the mean ± s.e.m. ($n \geq 150$ from three independent experiments). *$P < 0.05$ versus control siRNA-transfected cells, as calculated by one-way ANOVA with Dunnett's post-test.

GC1 is dispensable for EGF-mediated upregulation of clathrin-independent endocytosis

Next, to examine whether GC1 participates in the regulation of endocytosis in the context of EGF signaling, I first evaluated the effect of EGF on dextran uptake. As shown in **Figure 14A**, EGF increased the amount of internalized dextran. In consistent with the previous data in this thesis, expression of GC1 reduced dextran uptake at a basal level; however, in the presence of EGF, it was upregulated to the levels similar to that in control (**Figure 14A**). Moreover, remarkable additive effect of EGF on dextran uptake could be observed in GC1-knockdown cells (**Figure 14B**). Therefore, GC1 plays a role in the regulation of clathrin-independent endocytosis, but might be dispensable for its EGF-mediated regulation.

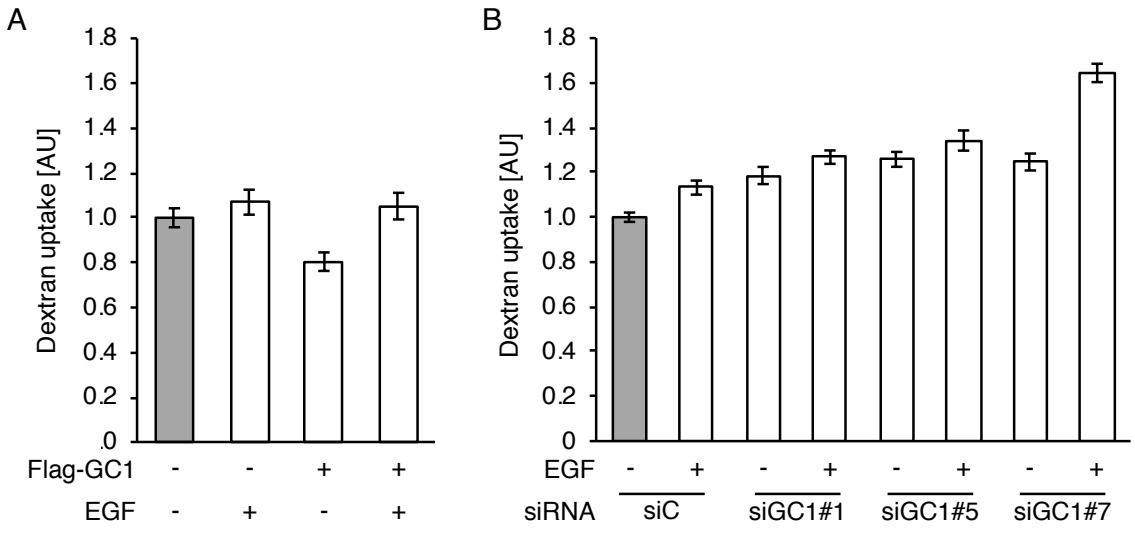

Figure 14. GC1 is dispensable for EGF-mediated regulation of clathrin-independent endocytosis

(**A** and **B**) A431 cells were transfected with a control vector or an expression vector encoding FLAG-GC1 for 24 hours (**A**) or transfected either siC or siGC1 for 72 hours (**B**). The cells were serum starved for 4 hours and then stimulated by EGF for 20 minutes or left untreated, followed by incubation with Alexa Fluor 546-labeled dextran for 10 minutes at 37°C. Total fluorescence intensities within the cells were quantified and plotted. Data are presented as the mean ± s.e.m. ($n \geq 20$ from one experiment (**A**), or $n \geq 100$ from one experiment (**B**)).

Knockdown of GC1 affected mitochondrial functions and morphology

I examined the effect of GC1 on mitochondrial functions, namely pH, membrane potential, and ATP concentration, as well as on morphology. pH in mitochondrial matrix in living cells was monitored with the use of a fluorescent protein-based pH indicator, which consists of pHluorin, a pH-sensitive variant of GFP (Orij et al., 2009), and mKate2, a pH-resistant far-red fluorescent protein (Katayama et al., 2008), in combination with the mitochondria marker protein mito. First, I confirmed that EGF stimulation did not affect the pH in mitochondria (**Figure 15A**). Under this condition, the ratio of fluorescence intensities of pHluorin and mKate2 was increased in GC1-knockdown cells (**Figure 15B**) after EGF stimulation, indicating that GC1 maintains pH homeostasis in the mitochondrial matrix in the presence of EGF.

I also examined whether knockdown of GC1 affects mitochondrial ATP concentration by using mitoATeam 1.03, a FRET-based ATP indicator targeted in the mitochondrial matrix

(Imamura et al., 2009), the emission ratio (FRET/CFP) of which positively correlates with ATP concentration. EGF stimulation did not affect ATP concentration in the mitochondria (**Figure 16A**). Moreover, no overt difference between control and GC1-knockdown cells was observed irrespective of the presence or absence of EGF (**Figure 16B**).

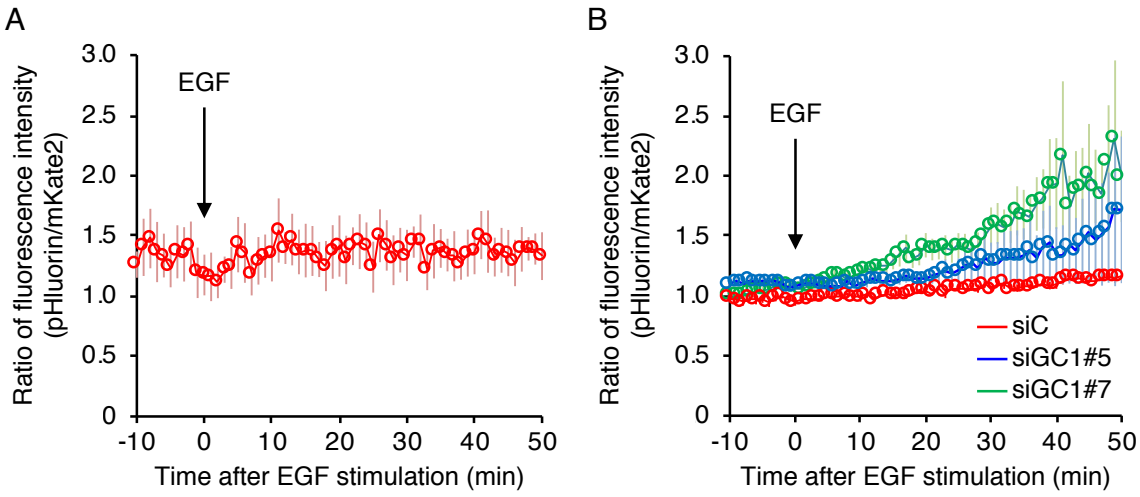

Figure 15. Mitochondrial pH was increased after EGF stimulation in GC1-knockdown cells

(**A**) A431 cells expressing mito-pHlourin-mKate2 were serum starved for 4 hours and subjected to time-lapse microscopy. At time 0 minute, the cells were stimulated by EGF. Fluorescence intensities of GFP and RFP in the mitochondria were quantified. The ratio of the fluorescence intensity of GFP to that of RFP was plotted. ($n \geq 5$ from one experiment).

(**B**) A431 cells were transfected with either siC or siGC1 for 48 hours. The cells were further transfected with mito-pHlourin-mKate2 for 24 hours. Time-lapse observation was performed, and the ratio was plotted. ($n \geq 4$ from one experiment).

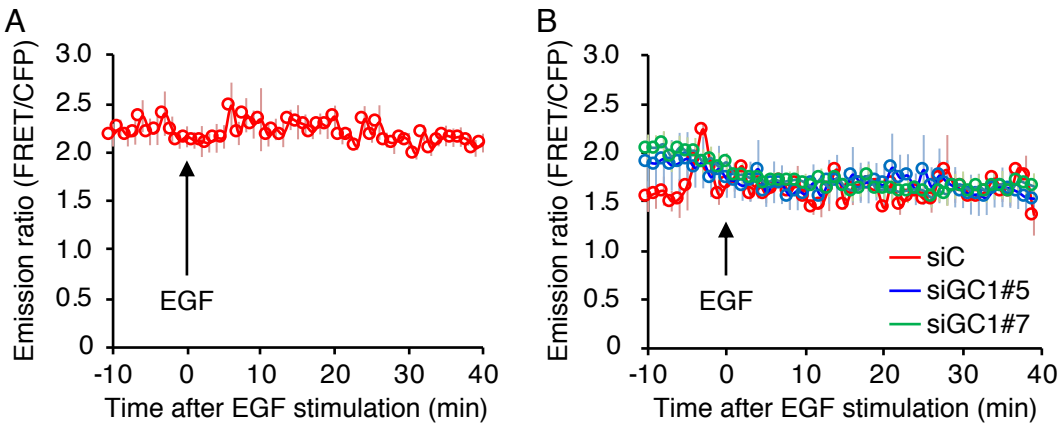

Figure 16. Mitochondrial ATP was not changed in GC1-knockdown cells

(**A**) A431 cells expressing mitoATeam 1.03 were serum starved for 4 hours, and subjected to time-lapse microscopy. At time 0 minute the cells were stimulated with EGF. The fluorescence intensities of CFP and FRET in the mitochondria were quantified and the FRET/CFP emission ratio was plotted ($n \geq 5$ from one experiment).

(**B**) A431 cells were transfected with either siC or siGC1 for 48 hours, the cells were further transfected with mitoATeam 1.03. Time-lapse observation was performed, and the emission ratio was calculated and plotted ($n \geq 4$ from one experiment).

Finally I checked the mitochondrial membrane potential in GC1-knockdown cells by using TMRM, a probe for mitochondrial membrane potential. Quantitative data on the fluorescence image of TMRM-treated cells showed that GC1-knockdown decreased the membrane potential of the mitochondria (**Figure 17A**). Mitochondrial morphology in GC1 knockdown cells was also investigated by using the mitochondria labeling dye MitoTrackerTM Red CMXRos (**Figure 17B**, left panels). Compared to control cells, GC1-knockdown cells displayed mitochondrial fragmentation (**Figure 17B**, right panel). Thus, GC1 knockdown induced mitochondrial fragmentation, possibly due to decreased membrane potential (Ishihara et al., 2003).

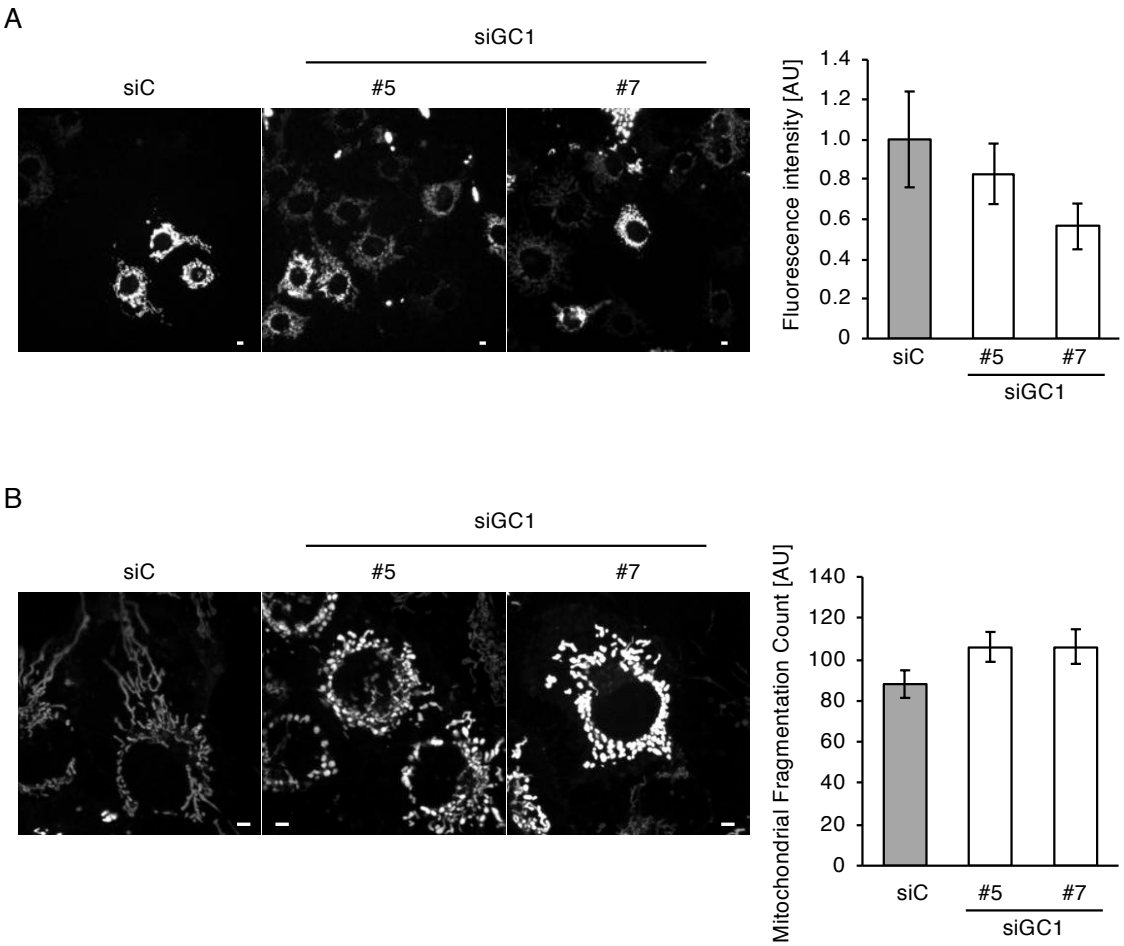

Figure 17. GC1 depletion decreased the mitochondrial membrane potential and promoted mitochondrial fragmentation

(**A** and **B**) A431 cells were transfected with either siC or siGC1. After 72 hours, the cells were treated with TMRM for 30 minutes (**A**), or MitoTracker™ Red CMXRos for 10 minutes (**B**) Representative images were shown. Bars, 10 μm. Total fluorescence intensity within cells (**A**), or Mitochondrial Fragmentation Count (**B**) was quantified and plotted. Data are presented as the mean ± s.e.m. ($n \geq 90$ (**A**), or $n \geq 10$ (**B**) from one experiment).

DISCUSSION

In this study, I investigated the function of GC1, which was identified from screening of binding partners of RAPEL, and revealed that it negatively regulates the endosomal translocation of Ras-PI3K complex, clathrin-independent endocytosis, and endosome maturation. In addition, GC1 was found to positively regulate clathrin-dependent endocytosis. To the best of my knowledge, no studies so far demonstrated the involvement of GC1 in the endocytic process; thus, I here provide a novel role of GC1 in the regulation of clathrin-independent endocytosis and endosome maturation through the Ras-PI3K localization in early endosomes. I also showed that the N-terminal region of GC1 is responsible for binding with RAPEL, whereas its C-terminus region dictates the mitochondrial localization (**Figures 6B** and **6C**). Because no functional domain, except for the region important for transporter function (Fiermonte et al., 2002), of GC1 has been reported as far as I am aware, such determination will be of great help in elucidating the molecular mechanisms through which GC1 regulates cellular phenomena, including endocytosis.

So far, the subcellular localization of GC1 has not been examined extensively compared to other member of SLC25 family proteins. Casimir, et al. demonstrated that GC1 is localized in the mitochondria in insulin-secreting β-cell by immunofluorescence assay (Casimir et al., 2009). In that study, it was also shown that GC1 resides in the inner membrane of mitochondria by electron microscopy (Casimir et al., 2009). On the other hand, I found that GC1 localizes in both the inner and outer membranes of mitochondria by using the mega-mitochondria method (**Figure 5**). The difference in the localization of GC1 between the previous report by Casimir group and my result might be due to the difference in the experimental conditions (fixed or living), or in the cell types used in the studies. In either case, GC1 on the mitochondrial outer membrane can directly interact with RAPEL and thereby participates in the regulation of endocytosis.

Voltage-dependent anion channel 2 (VDAC2), a pore-forming mitochondrial outer membrane protein, is one of the first identified factors that interact with RAPEL of PI3K. This protein upregulates clathrin-independent endocytosis and endosomal maturation through the formation of a mitochondria-endosome contact site (manuscript in preparation). In contrast, another mitochondrial outer membrane protein GC1 has been revealed as a negative regulator of clathrin-independent endocytosis and endosome maturation in this study. Such opposite effects of these two mitochondrial proteins on endocytosis might be accounted for by the differences in their functions (e.g. substrate transported through the pores) or in their

interacting molecules. VDAC2 is known to form a complex with adenine nucleotide translocator (ANT), an inner mitochondrial membrane protein (Vyssokikh and Brdiczka, 2003), and through the complex, it transports substances such as cytochrome C (Vyssokikh and Brdiczka, 2003). It is worth mentioning that ANT is also identified as a RAPEL-binding protein (unpublished data). Although no interacting protein of GC1 has been reported so far, it might be possible that, in analogy to VDAC2, GC1 functions through the macromolecule formation with inner mitochondrial membrane proteins. Indeed, several SLC25 proteins are reported to interact with other mitochondrial proteins (Gutiérrez-Aguilar and Baines, 2013). Screening of the inner mitochondrial proteins that bind to GC1 would be important to fully understand the molecular mechanism through which GC1 regulates endocytosis.

Given that purified GC1 embedded in liposomes displays outside-in unidirectional transport activity of glutamate along with H^+ and the rate of glutamate uptake is accelerated upon an increase in the proton concentration (Gutiérrez-Aguilar and Baines, 2013; Bradford and McGivan, 1973; Fiermonte et al., 2002), it is possible that the mitochondrial GC1 plays a role in regulating the endosome maturation by controlling H^+ influx into the mitochondria. It was to my surprise that GC1 knockdown increased the pH in mitochondria, only in the presence of EGF (**Figure 15B**). This raises the possibility that GC1 maintains pH homeostasis in the mitochondrial matrix against environmental perturbations that induce H^+ outflux from mitochondria through an unknown transporter(s). Here, I thereby propose a model for GC1-mediated regulation of endocytosis (**Figure 18**). (1) The Ras-PI3K complex is translocated from the plasma membrane to endosomes in an EGF-dependent manner through tethering factors such as VDAC2 and localized in very close proximity to the mitochondria. (2) GC1 is activated via RAPEL interaction and symports H^+ and glutamate from the cytosol to mitochondrial matrix, resulting in the low concentration of H^+ at the mitochondria-endosome contact site. (3) The H^+ transport from the contact site to the endosome through V-ATPase is decreased due to the low H^+ concentration, which collectively delays the endosome maturation.

To support the above model, further experimental verification will be required. For example, I have not evaluated changes in pH and influx of glutamate at the mitochondria-endosome contact site. Measurement of glutamate concentration in living cells with high resolution will be needed to do so. In addition, in order to determine whether the interaction between GC1 and RAPEL, rescue experiments by using GC1 mutants that cannot bind to RAPEL in GC1-kockdown cells should be performed. Furthermore, once critical amino acid residue(s) for

glutamate/H^+ transport would be identified, requirement for transport activity of GC1 in the regulation of endocytosis will be clarified through similar rescue experiments with the use of GC1 mutants with amino acid substitution at those sites.

To my surprise, I have found that GC1 functions not only as a negative regulator of clathrin-independent endocytosis, but also as a positive regulator of clathrin-dependent endocytosis. Although it is completely unknown how GC1 plays a dual role in the regulation of both pathways, it might be possible that GC1 regulates the "switching" of the endocytic pathways. For example, it is well known that under the suppression of clathrin-dependent endocytosis, through which influenza virus is internalized into host cells under normal conditions, it still enters into cells via clathrin-independent endocytosis (Fujioka et al., 2013; Chen and Zhuang, 2008; Rust et al., 2004; de Vries et al., 2011). Therefore, it might be worth elucidating the mechanism through which GC1 undergoes "pathway switching" between clathrin-dependent and clathrin-independent endocytosis under pathological conditions.

It is also possible that GC1 indirectly affects endocytosis through mitochondrial dysfunction. Indeed, GC1 knockdown resulted in decreased membrane potential and increased fragmentation of mitochondria (**Figure 17**), which might be consistent with evidence that a decrease in mitochondrial membrane potential shifts the mitochondrial morphology towards fragmentation (Ishihara et al., 2003). In contrast, GC1 knockdown displayed no significant impact on mitochondrial pH and ATP concentration (**Figures 15** and **16**). These results are controversial because the rate of ATP synthesis exponentially increases depending on the extent of depolarization of membrane potential (Dimroth et al., 2000). It would be critical to answer the question whether the dysfunction of mitochondria caused by GC1-knockdown upregulates endocytosis in the future study.

GC1 is expressed in a variety of human tissues and specifically enriched in the brain, liver, pancreas, and testes (Fiermonte et al., 2002; Molinari et al., 2005). Interestingly, it is reported that somatic missense mutations in GC1 gene, which have been identified by genetic mapping on patients with epileptic encephalopathy, display decreased activity in glutamate transport across a liposomal membrane (Cohen et al., 2014; Molinari et al., 2005; Poduri et al., 2013). Accordingly, the involvement of glutamate transporters at the plasma membrane or ER in the development of epilepsy is previously reported (Stafstrom, 2004); however, the mechanism through which the dysfunction of mitochondrial GC1 leads to the neuronal disorder is still unknown. On the other hand, a class of epilepsies are accounted for by dysfunction of endocytosis. For example, mutation in dynamin is found in epileptic encephalopathy

(Consortium et al., 2013; Wang et al., 2017), which results in the suppressed uptake of ligands such as transferrin (Dhindsa et al., 2015). Beyond neuronal disorders, GC1 in colorectal cancer cells with K-Ras mutation is upregulated and promotes cell proliferation and migration by upregulating the synthesis of aspartate derived from glutamine (Li et al., 2017; Wong et al., 2016). Given that endocytosis is reported to suppress cancer cell proliferation and invasion (Holst et al., 2017), overexpression of GC1 might promote such cancer cell malignancy through the inhibition of trafficking pathways. Thus, it might be worth exploring the involvement of GC1 in pathogenesis of diseases, including endocytosis-related diseases, in the future.

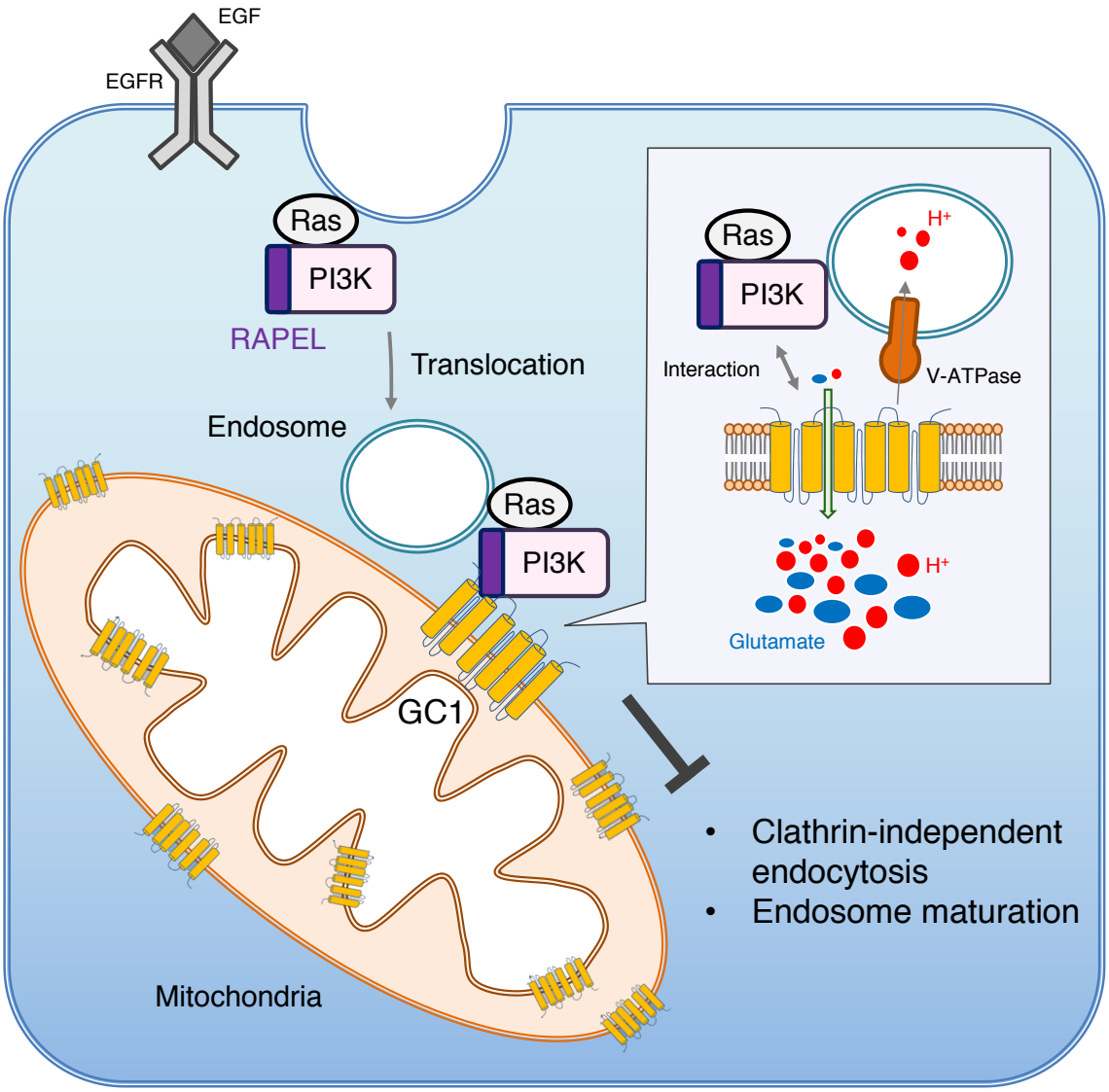

Figure. 18 Summary of this study

CONCLUSION

In this study, I have demonstrated that:

1. GC1 interacts with the RAPEL of PI3K.
2. GC1 is localized in the outer membrane of mitochondria.
3. GC1 negatively regulates Ras-PI3K translocation to the endosome.
4. GC1 suppresses endosomal acidification and clathrin-independent endocytosis
5. GC1 positively regulates clathrin-dependent endocytosis

GC1 was firstly identified in 2002 as a glutamate/proton symporter in the mitochondria. To date, there are no reports regarding the function of GC1 in membrane trafficking, namely endocytosis and endosomal acidification. Therefore, as far as I am aware, this is a first study that GC1 is implicated in the regulation of endocytosis. In addition, GC1 is demonstrated to play a two-sided role in the regulation of endocytosis: i.e. it regulated clathrin-dependent endocytosis and -independent endocytosis positively and negatively respectively. Given that extracellular substances, including influenza A virus, are reported to be internalized into cells via redundant pathways, such GC1 function might provide telling clues about how switching of endocytosis pathway is regulated.

On the other hand, the molecular mechanism through which GC1 regulates endocytosis has yet to be determined. Specifically, requirement for glutamate transport activity in the regulation of endocytosis is totally unknown. Visualization of spatiotemporal dynamics of local glutamate and proton concentrations with the use of fluorescent protein-biosensors would be of great help to elucidate this issue. Alternatively, once a mutant, of which transport activity is eliminated, will gain insight into the issue more directly. In addition, although the region bound to RAPEL has been revealed, the amino acid(s) that is critical for the binding has not been identified. Similarly, the C-terminal half of GC1 was demonstrated to dictate its mitochondrial localization; nevertheless, there exists no consensus sequence for targeting to this organelle. Through identification of the minimum sequence that governs these phenomena, it will be clarified whether GC1 binding to RAPEL or localizing to the mitochondrial is essential for GC1-mediated regulation of endocytosis.

In this study, I mainly focused on the role of GC1 in physiological condition. Given that GC1 has been implicated in the pathogenesis of diseases, including epilepsy and malignant tumors,

it will be worth analyzing the function of GC1 in the context of pathophysiology of diseases in the future.

ACKNOWLEDGMENTS

I would like to express my sincere thanks and gratitude to my respected supervisor Professor Yusuke Ohba from Department of Cell Physiology, Faculty of Medicine and Graduate School of Medicine, Hokkaido University, Japan for accepting me into the PhD program in his laboratory and providing his intellectual guidance, continuous encouragement, valuable suggestions, and outstanding inspirations throughout my PhD study.

I want to thank the Ministry of Education, Culture, Sports, Science and Technology (MEXT), Government of Japan for providing me Super Global MEXT (SG MEXT) scholarships during my graduate studies at Hokkaido University.

I wish to express my sincere gratitude to Dr. Yoichiro Fujioka, Lecturer, Department of Cell Physiology, Faculty of Medicine and Graduate School of Medicine, Hokkaido University, Japan for providing his incredible guidance in my research as well as in the analyses of laboratory results and thesis writing. I highly appreciate the untiring efforts of Dr. Aiko Yoshida and Dr. Aya O. Satoh for helping me for the preparation of this thesis and manuscript.

I want to thank Professor Hiroyuki Noji from The University of Tokyo for kindly providing mitoATeam 1.03 for my experiment.

I am thankful to all the members of Department of Cell Physiology, Faculty of Medicine and Graduate School of Medicine, Hokkaido University, Japan for their enormous support, guidance, and company during my graduate studies.

I want to express my sincere thanks to my husband Dr. Sarad Paudel and my son Mr. Taapas Paudel for their outstanding support during my studies. Finally, I would like to thank my parents Govind Prasad Atreya, Shuka Dev Nepal, Maya Devi Paudel, Arati Devi Nepal and all of my family members for their unconditional support, inspiration and blessings throughout my study here at Hokkaido University.

DISCLOSURE OF CONFLICT OF INTEREST

No potential conflict of interest to disclosure.

REFERENCES

Ascano, M., Bodmer, D., and Kuruvilla, R. (2012). Endocytic trafficking of neurotrophins in neural development. Trends Cell Biol. *22*, 266–273.

Bacci, A., Sancini, G., Verderio, C., Armano, S., Pravettoni, E., Fesce, R., Franceschetti, S., and Matteoli, M. (2002). Block of Glutamate-Glutamine Cycle Between Astrocytes and Neurons Inhibits Epileptiform Activity in Hippocampus. J. Neurophysiol. *88*, 2302–2310.

Balleza, E., Kim, J.M., and Cluzel, P. (2018). Systematic characterization of maturation time of fluorescent proteins in living cells. Nat. Meth. *15*, 47–51.

Boguski, M.S., and McCormick, F. (1993). Proteins regulating Ras and its relatives. Nature *366*, 643–654.

Bos, J.L. (1997). Ras-like GTPases. Biochim. Biophys. Acta. *1333*, 19–31.

Boyartchuk, V.L., Ashby, M.N., and Rine, J. (1997). Modulation of Ras and a-factor function by carboxyl-terminal proteolysis. Science *275*, 1796–1800.

Bradford, N.M., and McGivan, J.D. (1973). Quantitative characteristics of glutamate transport in rat liver mitochondria. Biochem. J. *134*, 1023–1029.

Campbell, S.L., Khosravi-Far, R., Rossman, K.L., Clark, G.J., and Der, C.J. (1998). Increasing complexity of Ras signaling. Oncogene *17*, 1395–1413.

Casimir, M., Lasorsa, F.M., Rubi, B., Caille, D., Palmieri, F., Meda, P., and Maechler, P. (2009). Mitochondrial glutamate carrier GC1 as a newly identified player in the control of glucose-stimulated insulin secretion. J. Biol. Chem. *284*, 25004–25014.

Castellano, E., and Santos, E. (2011). Functional specificity of ras isoforms: so similar but so different. Genes Cancer *2*, 216–231.

Chen, C., and Zhuang, X. (2008). Epsin 1 is a cargo-specific adaptor for the clathrin-mediated endocytosis of the influenza virus. Proc. Natl Acad. Sci. USA *105*, 11790–11795.

Chen, M.W., Wu, X.J. (2018). SLC25A22 Promotes Proliferation and Metastasis of Osteosarcoma Cells via the PTEN Signaling Pathway. Technol. Cancer Res. Treat. *17*, 1–10.

Chiu, V.K., Bivona, T., Hach, A., Sajous, J.B., Silletti, J., Wiener, H., Johnson, R.L., Cox, A.D., and Philips, M.R. (2002). Ras signalling on the endoplasmic reticulum and the Golgi. Nat. Cell Biol. *4*, 343–350.

Christoforidis, S., Miaczynska, M., Ashman, K., Wilm, M., Zhao, L., Yip, S.C., Waterfield, M.D., Backer, J.M., and Zerial, M. (1999). Phosphatidylinositol-3-OH kinases are Rab5 effectors. Nat. Cell Biol. *1*, 249–252.

Cohen, R., Basel-Vanagaite, L., Goldberg-Stern, H., Halevy, A., Shuper, A., Feingold-Zadok, M., Behar, D.M., and Straussberg, R. (2014). Two siblings with early infantile myoclonic encephalopathy due to mutation in the gene encoding mitochondrial glutamate/H+ symporter SLC25A22. Eur. J. Paediatric Neurol. *18*, 801–805.

Conner, S.D., and Schmid, S.L. (2003). Regulated portals of entry into the cell. Nature *422*, 37–44.

Consortium, E., Project, E.P.G., Consortium, E., and Project, E.P.G. (2013). De novo mutations in epileptic encephalopathies. Nature *501*, 217–221.

Das, A., Nag, S., Mason, A.B., and Barroso, M.M. (2016). Endosome-mitochondria interactions are modulated by iron release from transferrin. J. Cell Biol. *214*, 831–845.

Day, R.N., and Schaufele, F. (2008). Fluorescent protein tools for studying protein dynamics in living cells: a review. J. Biomed. Opt. *13*, 031202.

de Vries, E., Tscherne, D.M., Wienholts, M.J., Cobos-Jiménez, V., Scholte, F., García-Sastre, A., Rottier, P.J.M., de Haan, C.A.M. (2011). Dissection of the Influenza A Virus Endocytic Routes Reveals Macropinocytosis as an Alternative Entry Pathway. PLoS pathog. *7*, e1001329.

Dhindsa, R.S., Bradrick, S.S., Yao, X., Heinzen, E.L., Petrovski, S., Krueger, B.J., Johnson, M.R., Frankel, W.N., Petrou, S., Boumil, R.M., et al. (2015). Epileptic encephalopathy-causing mutations in DNM1 impair synaptic vesicle endocytosis. Neurol. Genet. *1*, 4–10.

Dimroth, P., Kaim, G., and Matthey, U. (2000). Crucial role of the membrane potential for ATP synthesis by F(1)F(o) ATP synthases. J. Exp. Biol. *203*, 51–59.

Downward, J. (1992). Regulation of p21ras by GTPase activating proteins and guanine nucleotide exchange proteins. Curr. Opin. Genet. Dev. *2*, 13–18.

Fiermonte, G., Palmieri, L., Todisco, S., Agrimi, G., Palmieri, F., and Walker, J.E. (2002). Identification of the mitochondrial glutamate transporter. Bacterial expression, reconstitution, functional characterization, and tissue distribution of two human isoforms. J. Biol. Chem. *277*, 19289–19294.

Frankel, P., Aronheim, A., Kavanagh, E., Balda, M.S., Matter, K., Bunney, T.D., and Marshall, C.J. (2005). RalA interacts with ZONAB in a cell density-dependent manner and regulates its transcriptional activity. EMBO J. *24*, 54–62.

Friedman, J.R., Dibenedetto, J.R., West, M., Rowland, A.A., and Voeltz, G.K. (2013). Endoplasmic reticulum-endosome contact increases as endosomes traffic and mature. Mol. Biol. Cell *24*, 1030–1040.

Frigerio, F., Casimir, M., Carobbio, S., and Maechler, P. (2008). Tissue specificity of mitochondrial glutamate pathways and the control of metabolic homeostasis. Biochim. Biophys. Acta. *1777*, 965–972.

Fujioka, Y., Nishide, S., Ose, T., Suzuki, T., Kato, I., Fukuhara, H., Fujioka, M., Horiuchi, K., Satoh, A.O., Nepal, P., et al. (2018). A Sialylated Voltage-Dependent Ca2+ Channel Binds Hemagglutinin and Mediates Influenza A Virus Entry into Mammalian Cells. Cell Host and Microbe *23*, 809–818.

Fujioka, Y., Satoh, A.O., Horiuchi, K., Fujioka, M., Tsutsumi, K., Sasaki, J., Nepal, P., Kashiwagi, S., Paudel, S., Nishide, S., et al. (2019). A Peptide Derived from Phosphoinositide 3-kinase Inhibits Endocytosis and Influenza Virus Infection. Cell. Struct. Funct. *44*, 61–74.

Fujioka, Y., Tsuda, M., Hattori, T., Sasaki, J., Sasaki, T., Miyazaki, T., and Ohba, Y. (2011). The Ras-PI3K signaling pathway is involved in clathrin-independent endocytosis and the internalization of influenza viruses. PLoS ONE *6*, e16324.

Fujioka, Y., Tsuda, M., Nanbo, A., Hattori, T., Sasaki, J., Sasaki, T., Miyazaki, T., and Ohba, Y. (2013). A Ca^{2+}-dependent signalling circuit regulates influenza A virus internalization and infection. Nat. Commun. *4*, 2763–13.

Giedt, R.J., Feruglio, P.F., Pathania, D., Yang, K.S., Kilcoyne, A., Vinegoni, C., Mitchison, T.J., and Weissleder, R. (2016). Computational imaging reveals mitochondrial morphology as a biomarker of cancer phenotype and drug response. Sci. Rep. *6*, 32985.

Goubert, E., Mircheva, Y., Lasorsa, F.M., Melon, C., Profilo, E., Sutera, J., Becq, H., Palmieri, F., Palmieri, L., Aniksztejn, L., et al. (2017). Inhibition of the Mitochondrial Glutamate Carrier SLC25A22 in Astrocytes Leads to Intracellular Glutamate Accumulation. Front. Cell. Neurosci. *11*, 169–15.

Gutiérrez-Aguilar, M., and Baines, C.P. (2013). Physiological and pathological roles of mitochondrial SLC25 carriers. Biochem. J. *454*, 371–386.

Hall, A., and Nobes, C.D. (2000). Rho GTPases: molecular switches that control the organization and dynamics of the actin cytoskeleton. Phil. Trans. R. Soc. B *355*, 965–970.

Hamasaki, M., Furuta, N., Matsuda, A., Nezu, A., Yamamoto, A., Fujita, N., Oomori, H., Noda, T., Haraguchi, T., Hiraoka, Y., et al. (2013). Autophagosomes form at ER-mitochondria contact sites. Nature *495*, 389–393.

Hancock, J.F., Cadwallader, K., Paterson, H., and Marshall, C.J. (1991). A CAAX or a CAAL motif and a second signal are sufficient for plasma membrane targeting of ras proteins. EMBO J. *10*, 4033–4039.

Hancock, J.F., Magee, A.I., Childs, J.E., and Marshall, C.J. (1989). All ras proteins are polyisoprenylated but only some are palmitoylated. Cell *57*, 1167–1177.

Heidler, J., Al-Furoukh, N., Kukat, C., Salwig, I., Ingelmann, M.-E., Seibel, P., Krüger, M., Holtz, J., Wittig, I., Braun, T., et al. (2011). Nitric oxide-associated protein 1 (NOA1) is necessary for oxygen-dependent regulation of mitochondrial respiratory complexes. J. Biol. Chem. *286*, 32086–32093.

Holst, M.R., Vidal-Quadras, M., Larsson, E., Song, J., Hubert, M., Blomberg, J., Lundborg, M., Landström, M., and Lundmark, R. (2017). Clathrin-Independent Endocytosis Suppresses Cancer Cell Blebbing and Invasion. Cell Rep. *20*, 1893–1905.

Huotari, J., and Helenius, A. (2011). Endosome maturation. EMBO J. *30*, 3481–3500.

Imamura, H., Nhat, K.P.H., Togawa, H., Saito, K., Iino, R., Kato-Yamada, Y., Nagai, T., and Noji, H. (2009). Visualization of ATP levels inside single living cells with fluorescence resonance energy transfer-based genetically encoded indicators. Proc. Natl Acad. Sci. USA *106*, 15651–15656.

Ishihara, N., Jofuku, A., Eura, Y., and Mihara, K. (2003). Regulation of mitochondrial morphology by membrane potential, and DRP1-dependent division and FZO1-dependent fusion reaction in mammalian cells. Biochemi. Biophys. Res. Commun. *301*, 891–898.

Jean, S., and Kiger, A.A. (2014). Classes of phosphoinositide 3-kinases at a glance. J. Cell Sci. *127*, 923–928.

Katayama, H., Yamamoto, A., Mizushima, N., Yoshimori, T., and Miyawaki, A. (2008). GFP-like proteins stably accumulate in lysosomes. Cell. Struct. Funct. *33*, 1–12.

Kunji, E.R.S., and Harding, M. (2003). Projection structure of the atractyloside-inhibited mitochondrial ADP/ATP carrier of Saccharomyces cerevisiae. J. Biol. Chem. *278*, 36985–36988.

Li, X., Chung, A.C.K., Li, S., Wu, L., Xu, J., Yu, J., Wong, C., and Cai, Z. (2017). LC-MS-based metabolomics revealed SLC25A22 as an essential regulator of aspartate-derived amino acids and polyamines in KRAS-mutant colorectal cancer. Oncotarget *8*, 101333–101344.

Lowy, D.R., and Willumsen, B.M. (1993). Function and regulation of ras. Annu. Rev. Biochem. *62*, 851–891.

Mayor, S., and Pagano, R.E. (2007). Pathways of clathrin-independent endocytosis. Nat. Rev. Mol. Cell Biol. *8*, 603–612.

Mesmin, B. (2016). Mitochondrial lipid transport and biosynthesis: A complex balance. J. Cell Biol. *214*, 9–11.

Molinari, F., Kaminska, A., Fiermonte, G., Boddaert, N., Raas-Rothschild, A., Plouin, P., Palmieri, L., Brunelle, F., Palmieri, F., Dulac, O., et al. (2009). Mutations in the mitochondrial glutamate carrier SLC25A22in neonatal epileptic encephalopathy with suppression bursts. Clin. Genet. *76*, 188–194.

Molinari, F., Raas-Rothschild, A., Rio, M., Fiermonte, G., Encha-Razavi, F., Palmieri, L., Palmieri, F., Ben-Neriah, Z., Kadhom, N., Vekemans, M., et al. (2005). Impaired mitochondrial glutamate transport in autosomal recessive neonatal myoclonic epilepsy. Am. J. Hum. Genet. *76*, 334–339.

Nakashima, S., Morinaka, K., Koyama, S., Ikeda, M., Kishida, M., Okawa, K., Iwamatsu, A., Kishida, S., and Kikuchi, A. (1999). Small G protein Ral and its downstream molecules regulate endocytosis of EGF and insulin receptors. EMBO J. *18*, 3629–3642.

Orij, R., Postmus, J., Beek, Ter, A., Brul, S., and Smits, G.J. (2009). In vivo measurement of cytosolic and mitochondrial pH using a pH-sensitive GFP derivative in Saccharomyces cerevisiae reveals a relation between intracellular pH and growth. Microbiology *155*, 268–278.

Palmieri, E.M., Spera, I., Menga, A., Infantino, V., Iacobazzi, V., and Castegna, A. (2014). Glutamine synthetase desensitizes differentiated adipocytes to proinflammatory stimuli by raising intracellular glutamine levels. FEBS Lett. *588*, 4807–4814.

Palmieri, F. (2004). The mitochondrial transporter family (SLC25): physiological and pathological implications. Pflugers Arch. *447*, 689–709.

Palmieri, F. (2014). Mitochondrial transporters of the SLC25 family and associated diseases: a review. J. Inherit. Metab. Dis. *37*, 565–575.

Palmieri, F., and Monné, M. (2016). Discoveries, metabolic roles and diseases of mitochondrial carriers: A review. Biochim. Biophys. Acta *1863*, 2362–2378.

Pebay-Peyroula, E., Dahout-Gonzalez, C., Kahn, R., Trézéguet, V., Lauquin, G.J.-M., and Brandolin, G. (2003). Structure of mitochondrial ADP/ATP carrier in complex with carboxyatractyloside. Nature *426*, 39–44.

Poduri, A., Heinzen, E.L., Chitsazzadeh, V., Lasorsa, F.M., Elhosary, P.C., LaCoursiere, C.M., Martin, E., Yuskaitis, C.J., Hill, R.S., Atabay, K.D., et al. (2013). SLC25A22 is a novel gene for migrating partial seizures in infancy. Ann. Neurol. *74*, 873–882.

Prior, I.A., Lewis, P.D., Mattos, C. (2012). A Comprehensive Survey of Ras Mutations in Cancer. Cancer Res. *72*, 2457–2467.

Rahman, M., Ham, H., Liu, X., Sugiura, Y., Orth, K., and Krämer, H. (2012). Visual neurotransmission in Drosophila requires expression of Fic in glial capitate projections. Nat. Neurosci. *15*, 871–875.

Rizzuto, R., De Stefani, D., Raffaello, A., and Mammucari, C. (2012). Mitochondria as sensors and regulators of calcium signalling. Nat. Rev. Mol. Cell Biol. *13*, 566–578.

Robbins, D.J., Cheng, M., Zhen, E., Vanderbilt, C.A., Feig, L.A., and Cobb, M.H. (1992). Evidence for a Ras-dependent extracellular signal-regulated protein kinase (ERK) cascade. Proc. Natl Acad. Sci. USA. *89*, 6924–6928.

Rowland, A.A., Chitwood, P.J., Phillips, M.J., and Voeltz, G.K. (2014). ER Contact Sites Define the Position and Timing of Endosome Fission. Cell *159*, 1027–1041.

Rust, M.J., Lakadamyali, M., Zhang, F., Zhuang, X. (2004). Assembly of endocytic machinery around individual influenza viruses during viral entry. Nat. Struct. Mol. Biol. *11*, 567–573.

Sheftel, A.D., Zhang, A.S., Brown, C., Shirihai, O.S., and Ponka, P. (2007). Direct interorganellar transfer of iron from endosome to mitochondrion. Blood *110*, 125–132.

Stafstrom, C.E. (2004). The role of glutamate transporters in developmental epilepsy: a concept in flux. Epilepsy Curr. *4*, 243–244.

Tsutsumi, K., Fujioka, Y., Tsuda, M., Kawaguchi, H., and Ohba, Y. (2009). Visualization of Ras-PI3K interaction in the endosome using BiFC. Cell. Signal. *21*, 1672–1679.

Vance, J.E. (1990). Phospholipid synthesis in a membrane fraction associated with mitochondria. J. Biol. Chem. *265*, 7248–7256.

Vance, J.E. (2014). MAM (mitochondria-associated membranes) in mammalian cells: lipids and beyond. Biochim. Biophys. Acta. *1841*, 595–609.

Vanhaesebroeck, B., Stephens, L., and Hawkins, P. (2012). PI3K signalling: the path to discovery and understanding. Nat. Rev. Mol. Cell Biol. *13*, 195–203.

Vojtek, A.B., and Der, C.J. (1998). Increasing complexity of the Ras signaling pathway. J. Biol. Chem. *273*, 19925–19928.

Vojtek, A.B., Hollenberg, S.M., and Cooper, J.A. (1993). Mammalian Ras interacts directly with the serine/threonine kinase Raf. Cell *74*, 205–214.

Vyssokikh, M.Y., and Brdiczka, D. (2003). The function of complexes between the outer mitochondrial membrane pore (VDAC) and the adenine nucleotide translocase in regulation of energy metabolism and apoptosis. Acta Biochim. Pol. *50*, 389–404.

Wang, C., and Youle, R.J. (2009). The role of mitochondria in apoptosis. Annu. Rev. Genet. *43*, 95–118.

Wang, J., Lin, Z.J., Liu, L., Xu, H.Q., Shi, Y.W., Yi, Y.H., He, N., and Liao, W.P. (2017). Epilepsy-associated genes. Seizure *44*, 11–20.

Wong, C.C., Qian, Y., Li, X., Xu, J., Kang, W., Tong, J.H., To, K.F., Jin, Y., Li, W., Chen, H., et al. (2016). SLC25A22 Promotes Proliferation and Survival of Colorectal Cancer Cells With KRAS Mutations and Xenograft Tumor Progression in Mice via Intracellular Synthesis of Aspartate. Gastroenterology *151*, 945–960.